Comparative osteology of the fossorial frogs of the genus *Synapturanus* (Anura, Microhylidae) with the description of three new species from the Eastern Guiana Shield

Fouquet Antoine [1, *], Leblanc Killian [1], Fabre Anne-Claire [2], Rodrigues Miguel T. [3], Menin Marcelo [4], Courtois Elodie A. [5], Dewynter Mael [6], Holting Monique [7, 8], Ernst Raffael [8], Peloso Pedro [9], Kok Philippe J. R. [2, 10]

[1] Univ Paul Sabatier, Lab Evolut & Diversite Biol, CNRS, IRD,UMR 5174, Batiment 4R1,118 Route Narbonne, F-31062 Toulouse 9, France.
[2] Nat Hist Museum, Dept Life Sci, London SW7 5BD, England.
[3] Univ Sao Paulo, Dept Zool, Inst Biociencias, Sao Paulo, SP, Brazil.
[4] Univ Fed Amazonas, Inst Ciencias Biol, Dept Biol, BR-69080900 Manaus, Amazonas, Brazil.
[5] IRD, LEEISA, Ctr Rech Montabo, 275 Route Montabo,BP 70620, Cayenne 97334, French Guiana.
[6] La Desiree, F-97351 Matoury, French Guiana.
[7] Leibniz Inst Anim Biodivers, Zool Res Museum Alexander Koenig, Adenauerallee 160, D-53113 Bonn, Germany.
[8] Senckenberg Nat Hist Collect Dresden, Museum Zool, Dresden, Germany.
[9] Univ Fed Para, Inst Ciencias Biol, R Augusto Correa 1, BR-66075110 Belem, Para, Brazil.
[10] Univ Lodz, Fac Biol & Environm Protect, Dept Ecol & Vertebrate Zool, 12-16 Banacha Str, PL-90237 Lodz, Poland.

* Corresponding author : Antoine Fouquet, email address : fouquet.antoine@gmail.com

Abstract :

The genus Synapturanus includes three nominal species of fossorial Amazonian frogs. A previous study combining molecular, morphological and acoustic data suggested that there may be six times more species than currently recognized. Herein we describe and name three of these new species and compare their osteology. Synapturanus zombie sp. nov. occurs in French Guiana and Amapa (Brazil), Synapturanus mesomorphus sp. nov. in Guyana and adjacent Venezuela, and Synapturanus ajuricaba sp. nov. in the northern part of the Brazilian states of Amazonas and Para. These species are readily differentiated from congeners by a combination of external morphological characters such as body size, development of fringes on fingers and coloration, by advertisement call variables, and by osteological traits. Along with osteological reinforcement of the skull, atlas and scapular region, the reduction of the size of phalanges, more developed fringes on fingers, smaller eyes and larger body size, altogether suggest an overall increase of the fossorial habits in the easternmost species. In contrast, the relatively conserved morphology of the posterior part of the body across the genus suggests that fossoriality mostly involves the anterior part. Furthermore, the fusion of tarsal bones in the species of the western clade may indicate locomotory adaptation to more epigean habits. (C) 2021 Elsevier GmbH. All rights reserved.

1. Introduction

Microhylidae is one of the largest family of amphibians, with a global distribution and a remarkable diversity of morphological and ecological traits. Within the Neotropics, microhylids represent 18% of the total number of described species (Frost, 2021) and belong to two major groups: Gastrophryninae Fitzinger, 1843, the most species rich subfamily with 81 species (Frost, 2021) distributed from southern North America to Argentina; and a species poor clade formed by the monotypic Adelastinae Peloso, Frost, Richards, Rodrigues, Donnellan, Matsui, Raxworthy, Biju, Lemmon, Lemmon, and Wheeler, 2016 and Otophryninae Wassersug and Pyburn, 1987. The latter subfamily is limited to two genera, each including three valid nominal species: *Otophryne* Boulenger, 1900 and *Synapturanus* Carvalho, 1954, all described from the Guiana Shield. Whereas *Otophryne* are epigean, diurnal, and ripicolous species with exotrophic tadpoles, *Synapturanus* are fossorial, nocturnal, associated with well drained soils of *terra-firme* (non-flooded) forests and have an endotrophic mode of development (Pyburn, 1975; Menin et al., 2007). The three known species of *Synapturanus*, (*S. mirandaribeiroi* Nelson and Lescure, 1975, *Synapturanus rabus* Pyburn, 1977, and *Synapturanus salseri* Pyburn, 1975) occur in the lowlands and seemingly have very brief and rare periods of calling activity (Nelson and Lescure, 1975; Ernst et al., 2005). Individuals have been observed in underground galleries and nuptial chambers, which they dig to deposit eggs that undergo endotrophic development (Nelson and Lescure, 1975; Pyburn, 1975, 1977; Menin et al., 2007). Although no direct observations have been reported, the overall morphology, and notably the shape of the snout and humerus, suggest a head-first, forward-burrowing, behavior (Keeffe and Blackburn, 2020; Fouquet et al., 2021). Overall, *Synapturanus* are poorly known, and the scarcity of basic data on their life-history and rarity in zoological collections is easily explained by their secretive lifestyle.

72   Using a combination of genetic, acoustic and morphological data, Fouquet et al.

73 (2021) demonstrated that the diversity in Otophryninae is largely underestimated. For

74 *Synapturanus*, for example, the study suggests that at least another 15 species could be

75 formally recognized. Such an underestimation of the species diversity in *Synapturanus* is

76 partly explained by the combination of (1) the difficulty to access many remote parts of

77 Amazonia; (2) the challenging task that collecting these markedly fossorial and secretive

78 species represents; (3) the scarcity of comprehensive acoustic, molecular and morphological

79 reference data, especially from topotypical material, rendering comparison and description

80 difficult; and (4) the prevalence of small and allopatric distributions of the different species

81 probably linked to low dispersal ability and specific ecological requirements.

82   The phylogenetic data in Fouquet et al. (2021) also demonstrated that three major

83 clades exist within *Synapturanus. Synapturanus salseri*, *S. mirandaribeiroi* and seven

84 additional candidate species form a clade occurring in the Guiana Shield as well as extending

85 into the southern part of the Amazon River basin. *Synapturanus rabus* and six candidate

86 species belong to a clade restricted to western Amazonia. The third clade is formed by two

87 unnamed candidate species from central Amazonia. *Synapturanus mirandaribeiroi* was

88 described based on specimens from Kanashen (also spelled "Konashen", Southern Guyana)

89 and was reported throughout the Guiana Shield (Nelson and Lescure, 1975; Pyburn, 1975;

90 Lima et al., 2006; Menin et al., 2007; Ávila-Pires et al., 2010; Barrio-Amorós et al., 2019), as

91 well as the right bank of the Rio Negro, in the Jaú National Park (Neckel-Oliveira and Gordo,

92 2004). However, genetic, morphological and acoustic variation across this range suggests that

93 some of these populations may not belong to *S. mirandaribeiroi*. The similarity between the

94 skull and humerus of the paratype (MNHN-RA-1974.0397) and that of specimens from

95 southwestern French Guiana, Suriname and the Manaus region, an area encompassing the

96 type locality of *S. mirandaribeiroi*, strongly suggests conspecificity (Fouquet et al., 2021).

97   Moreover, genetic data indicate that these specimens form a lineage related to populations

98   located in the southern part of the Amazon River basin (*Synapturanus* sp. "Purus" and

99   *Synapturanus* sp. "Tapajos") that are phenotypically distinct. However, they are also related

100   to a single specimen (*Synapturanus* sp. "Taboca") that is genetically albeit not

101   morphologically distinct from *S. mirandaribeiroi*. This specimen is from a locality (Taboca,

102   Amazonas, Brazil) also relatively close to Kanashen (ca. 310 km airline). Therefore, some

103   ambiguity remains whether all these populations belong to a single species, i.e., *S.*

104   *mirandaribeiroi*, or if the name *S. mirandaribeiroi* only applies to one of these two groups of

105   populations (Fouquet et al., 2021).

106   *Synapturanus salseri* was described from Vaupés, Colombia, and populations from

107   Brazil's Manaus region (Lima et al., 2006; Menin et al., 2007), Venezuela (Barrio-Amorós et

108   al., 2019), and Guyana (Kok and Kalamandeen, 2008) have also been tentatively assigned to

109   this taxon. Unfortunately, no DNA sequences unequivocally assignable to this taxon (i.e.,

110   from the type locality or its vicinity) have been made available yet (Peloso et al., 2016

111   included sequences labeled as "*S. salseri*", but these sequences belong to one of the unnamed

112   candidate species of Fouquet et al., 2021). Furthermore, the morphology of the skull and of

113   the humerus suggest that this name cannot be applied to any known populations outside of the

114   type locality (Fouquet et al., 2021).

115   Finally, *Synapturanus rabus* belongs to a clade formed by species from western

116   Amazonia displaying distinct calls (short notes) and morphology (elongated body and limbs)

117   (Fouquet et al., 2021).

118   Herein, we describe and name three of these new species, previously reported as

119   *Synapturanus* sp. "Eastern Guianas", *Synapturanus* sp. "Guyana" and *Synapturanus* sp.

120   "Manaus" (Fouquet et al., 2021), for which we could gather sufficient phylogenetic,

121   morphological (external and osteology) and acoustic evidence to diagnose the new taxa from

122   currently valid nominal species.

123

124   **2. Material and Methods**

125   *2.1. External morphology*

126   We examined 38 specimens of the new species (7 *S.* sp. "Eastern Guianas", 8 *S.* sp.

127   "Manaus", 23 *S.* sp. "Guyana") deposited in various zoological collections (Appendix A), and

128   compared them with specimens of the three named species of the genus, *S. mirandaribeiroi*,

129   *S. salseri*, and *S. rabus*, including type specimens and topotypical material (Table 1,

130   Appendix B). Among those specimens, 12 were included in the genetic dataset of Fouquet et

131   al. (2021) and are thus directly linked to candidate species. The other specimens were

132   assigned to one of the species based on morphological examination and on the geographic

133   proximity of their collecting locality relative to that of a genotyped specimen.

134   We measured 12 morphological variables on examined specimens, following Kok and

135   Kalamandeen (2008): snout-vent length (SVL); head length, from the corner of the mouth to

136   the tip of the snout (HL); head width at the level of the angle of jaws (HW); eye-to-naris

137   distance, from the anterior edge of the eye to the center of the naris (EN); internarial distance

138   (IN); horizontal eye diameter (ED); interorbital distance, representing the width of the

139   underlying frontoparietal (IO); forearm length, from the proximal edge of the palmar tubercle

140   to the outer edge of the flexed elbow (FAL); hand length, from the proximal edge of the

141   palmar tubercle to the tip of the Finger III (HAND); crus (tibiofibular) length, from the outer

142   edge of the flexed knee to the heel (TL); foot length, from the proximal edge of the inner

143   metatarsal tubercle to the tip of Toe IV (FL); and thigh length, from the vent opening to the

144   outer edge of the flexed knee (ThL).

145 *2.2. Bioacoustics*

146 We compiled call recordings of 11 males of the new species (4 *S*. sp. "Eastern Guianas", 5 *S*.

147 sp. "Manaus", 2 *S*. sp. "Guyana") from various available sources (see Fouquet et al., 2021),

148 and compared them to the calls of *S. mirandaribeiroi*, *S. rabus* and *S. salseri*. We followed a

149 call-centered approach and measured four call variables following those standardized in

150 Köhler et al. (2017): Note Length (NL), Dominant Frequency (DoF, which also corresponds

151 to the fundamental frequency in the genus; taken with a spectral slice over the entire note),

152 Delta Frequency (DeF) (difference in peak frequency between spectral slices taken over the

153 first and the last 0.015 s of the note), inter-note length (the silence between the end of one

154 note and the beginning of the next one). We measured temporal and spectral variables from

155 waveforms and spectrograms using Audacity v.2.4.1 (Audacity Team, 2020). These

156 recordings are heterogeneous in terms of length and quality. Calls recorded with high quality

157 are often single or in very low numbers per recording and we selected the ones with the best

158 quality to measure acoustic variables. When more than one good quality call was available

159 per recorded male, we used the average calculated across up to four measures.

160 *2.3. Osteology*

161 Fouquet et al. (2021) unraveled an extensive osteological (skull and humerus) variation

162 among candidate species using morphometric data from micro computed tomography scans

163 (μCT-scans). We expanded the study of this variation to the entire skeleton (skull, vertebral

164 column, pectoral and pelvic girdles) of (1) the three new species (1 male and 1 female of each

165 except in *S*. sp. "Manaus", for which only two females were available); (2) *Synapturanus*

166 *mirandaribeiroi* (1 male paratopotype and 1 male and 1 female recently collected); (3) *S*.

167 *salseri* (1 male paratopotype); (4) *S*. sp. "Ecuador", as a representative of the western clade (1

168 male and 1 female); and (5) *S*. sp. "Juami", as a representative of the central clade (1 male and

169 1 female) (Table 3). These μCT-scans were retrieved from www.morphosource.org

170   (Appendix C). Fourteen specimens used for osteological comparisons were also genotyped

171   and could thus be directly linked to the DNA-based species delimitation of Fouquet et al.

172   (2021).

173   Osteological descriptions are based on surfaces rendered in AVIZO using the 'phong'

174   renderer with a custom preset (available from the corresponding author upon request),

175   adjusted for each scan to reveal the skeleton but not the rest of the matrix. Scans with edge

176   and beam-hardening artefacts were refined using local thresholds, clipping planes with

177   Geomagic. Anatomic figures were constructed using image captures with MeshLab function

178   "snapshot" under an orthographic field of view. Measurements were taken from these models

179   using MeshLab measuring tool (Fig. S1). Osteological terminology follows Trueb (1968,

180   1973), with that of the carpals and tarsals following Fabrezi and Alberch (1996). Newly

181   obtained surface rendering of the scans are deposited at

182   http://morphosource.org/Detail/ProjectDetail/Show/project_id/254. Readers are advised that

183   micro-CT preparations are targeted to render osteology and do not render most of the

184   cartilage. Therefore, as too few specimens were available for clearing and staining, we opted

185   to omit cartilage descriptions from our skeletal descriptions and comparisons below.

186

187   **3. Results**

188

189   Herein, we formally describe and name three new species of *Synapturanus* previously

190   recognized in Fouquet et al. (2021) as *Synapturanus* sp. "Eastern Guianas", *Synapturanus* sp.

191   "Manaus" and *Synapturanus* sp. "Guyana". As the three new species are nested in the eastern

192   clade of Fouquet et al. (2021), along with *S. salseri*, *S. mirandaribeiroi* and four additional

193   putative new species, we rediagnose the first two species and comment upon relevant

194   information before formally describing the new taxa.

3.1. Taxonomic accounts

Members of the genus *Synapturanus* are mainly characterized by the following external features: (1) body stout, usually globular; (2) snout long, strongly protruding, projecting well beyond the end of the lower jaw; (3) tympanum usually concealed and only distinct anteroventrally; (4) nares oriented laterally, closer to the tip of the snout than to the eye; (5) loreal region strongly concave, grooved; (6) supratympanic fold running from the posterior corner of the eye, curving towards the axilla; (7) occipital (postcephalic) fold continuous with supratympanic fold; (8) gular fold continuous with occipital fold; (9) presence of a thoracic fold; (10) skin on dorsum smooth; (11) skin on venter smooth; (12) fingers short, relative length of fingers III > IV > II > I; (13) toes unwebbed, relative length of toes IV > III > V > II > I; (14) subarticular tubercles not visible on toes; (15) absence of vocal slits; (16) absence of vocal sac; (17) absence of maxillary teeth; and (18) glandular unpigmented supracarpal pad present in males (poorly visible in preservative).

3.1.1. Synapturanus mirandaribeiroi Nelson and Lescure, 1975

3.1.1.1. Holotype. MZUSP49981 an adult female collected by Craig E. Nelson and Gene A. Miller between the 17th and the 30th of July 1968 at Kanashen (a Waiwai Indian village and mission) on the Upper Essequibo River, Rupununi District, Guyana.

3.1.1.2. Allotype. AMNH90935, an adult male with the same data as the holotype.

3.1.1.3. Paratypes. A series of six males, five females, and two juveniles with the same data as the holotype, deposited as follows: AMNH90936–90943, MNHN-RA-1974.0397, National

220   Museum of Guyana (numbers not mentioned by Nelson and Lescure, 1975), and

221   UMMZ136147.

222

223   *3.1.1.4. Material examined.* MZUSP49981, AMNH90935, AMNH90937, MNHN-RA-

224   1974.0397 and the following 16 non type specimens referred to as *S. mirandaribeiroi*:

225   MNHN-RA-2020.0079–82, INPA-H10890, INPA-H11837, INPA-H11843, INPA-H11867,

226   INPA-H13169–70, INPA-H18572, INPA-H19781, INPA-H34023, INPA-H37891 (Appendix

227   B).

228

229   *3.1.1.5. Definition and diagnosis.* (1) medium-sized *Synapturanus* (average male SVL 29.1

230   mm [26.2–30.8, $n = 14$], female SVL 31.5 mm [28.6–34.4, $n = 3$]) (Fig. 1; Table 1); (2) head

231   dorsally convex in lateral view; (3) eyes small, slightly smaller than eye-naris distance; (4)

232   fingertips rounded; (5) subarticular tubercles not visible on fingers; (6) thenar tubercle large

233   and prominent, palmar tubercle indistinct; (7) Fingers II and III with preaxial fringe extending

234   towards the base of fingers in males and females; (8) toe tips slightly expanded on Toes III,

235   IV and V; (9) inner metatarsal tubercle small, ovoid and conspicuous, outer metatarsal

236   tubercle indistinct; (10) dorsal color pattern medium brown with abundant small spots (orange

237   in life, cream in preservative) forming a mottled pattern, a continuous stripe extends from the

238   snout along the canthus rostralis and upper eyelid to midway between eye and axilla; (11)

239   venter pearl white with sparse melanophores, throat color similar to dorsum in males and

240   females; (12) conspicuous depressions on the prootic and frontoparietal, sphenoid-nasal

241   bridge and septum highly ossified, phalanges I–II of Finger III shorter than metacarpal, tibiale

242   and fibulare only fused on extremities, axis processes with enlarged terminal parts and atlas

243   with a bulbous neural spine; (13) call consisting in a pulsed (5–8 fused pulses) note 0.130–

244   0.194 s in length with a downward frequency modulation (delta 22–234 Hz) and a dominant

245   frequency at 1.10–1.47 kHz (*n* = 9) (Table 2).

246

247   *3.1.1.6. Advertisement call.* Nine specimens calling from underground galleries were recorded

248   from a distance of about 2 m at air temperatures ranging from 22 to 24°C (temperatures in the

249   burrows unknown). Descriptive statistics of call parameters are presented in Table 2.

250   *Synapturanus mirandaribeiroi* emits single pulsed (5–8 fused pulses) notes (note length mean

251   = 0.166, range 0.130–0.194 s) every 6.56 s on average (range 4.10–11.60 s). The spectral

252   structure of the note has a developed harmonic structure and the dominant frequency is 1.25

253   kHz on average (range 1.10–1.47 kHz) with a strong downward modulation (ca. 0.02–0.23

254   kHz) (Fig. 1 and Table 2).

255

256   *3.1.1.7. Remarks.* The call recordings from Suriname (Voltzberg) and the Manaus region

257   (Brazil) are distinct despite the fact that these populations are closely related according to the

258   genetic data (Fouquet et al., 2021). The pulses are more pronounced, notes are longer, the

259   downward modulation is more marked and the dominant frequency is lower in the Suriname

260   population compared to the Brazilian populations. Therefore, we suspect that these

261   populations may not be conspecific, contradicting molecular data and suggesting that an in-

262   depth investigation is warranted. This observation adds to the ambiguity surrounding the

263   conspecificity with *S*. sp. "Taboca" and the absence of molecular and call data from the type

264   locality of *S. mirandaribeiroi*. Nevertheless, all these populations are closely related and

265   remain indistinguishable morphologically (external and internal) thus allowing diagnosis and

266   comparison with other species.

267   We doubt that the two specimens reported by Pyburn (1975) as co-occurring in

268   Vaupés with *S. salseri* belong to *S. mirandaribeiroi*. These specimens (UTA-A-3987, UTA-

269   A-4009) have SVL=37.0 and 35.0 mm, respectively, are much larger than males of *S.*

270   *mirandaribeiroi* (26.2–30.8 mm). Moreover, the specimens reported by Nelson and Lescure

271   (1975) from Taracuá, Brazil, on Rio Vaupés (Melin, 1941), a locality only 20 km east of

272   Timbo may be conspecific. Similarly, some of the specimens reported by Nelson and Lescure

273   (1975) as *S. mirandaribeiroi*, fortunately not included in the type series, in fact belong to *S.*

274   sp. "Eastern Guianas" (Alikéné), *S*. sp. "Manaus" (Oriximiná; Itapiranga) and *S*. sp. "Guyana"

275   (Demerara Falls and Kartabo according to Nelson and Lescure, 1975), that are described as

276   new hereafter.

277

278   *3.1.1.8. Habitat and natural history.* In French Guiana and Suriname, the species was found

279   in pristine mature *terra firme* forests, and notably often in sandy soils near inselbergs.

280   Vocalizations are more common during and immediately after rain showers and were heard

281   between November and December, i.e., during the beginning of the rainy season (Menin et

282   al., 2008). Menin et al. (2007) provided detailed information about the reproduction and

283   embryonic/larval development of this species from a population nearby Manaus, Amazonas,

284   Brazil. Two clutches contained six and nine eggs in burrows about 5–10 cm deep below the

285   soil surface; tadpoles hatched at stage 42 of Gosner (1960) (Menin et al., 2007). Nelson and

286   Lescure (1975) reported ants in the stomachs of one allotype and one specimen from New

287   River (Guyana).

288

289   *3.1.1.9. Distribution and conservation status. Synapturanus mirandaribeiroi* is known from

290   16 populations (Fig. 2), assuming conspecificity of the related populations mentioned above

291   and additional records from Brazil (Parque Estadual Rio Negro); Guyana (Onoro;

292   Shudikarwau – Nelson and Lescure, 1975); and Suriname (Fredberg – Dick Lock, pers. com.,

293   Oelemarie River; Lucie River – Ouboter and Jairam, 2012; Sipaliwini – Nelson, 1973;

294   Palumeu – Nelson and Lescure, 1975). Nelson and Lescure (1975) provided an additional

295   locality (Tung District at 610 m elevation in Guyana) that we could not locate. This range

296   encompasses a large portion of the Eastern Guiana Shield and includes several protected

297   areas. The species probably occurs in the northern part of the states of Amapá, Pará, and

298   Roraima, in Brazil. *Synapturanus mirandaribeiroi* is found between 100–400 m above sea

299   level (asl).

300   Although the number of known populations remains limited, we suggest the status of

301   this species to be considered as Least Concern according to IUCN criteria (IUCN, 2020). The

302   distribution of *S. mirandaribeiroi* strikingly mirrors the one of *Anomaloglossus stepheni*

303   (Vacher et al., 2017).

304

305   *3.1.2.1. Synapturanus salseri* Pyburn, 1975

306

307   *3.1.2.2. Holotype.* UTA-A-4011, an adult male collected by John K. Salser Jr. and William F.

308   Pyburn the 17th of June 1973 at Timbo, Vaupés, Colombia.

309

310   *3.1.2.3. Paratypes.* A series of 13 males and 6 juveniles collected with the holotype by Salser

311   and Pyburn between the 17th and the 29th of June 1973 and on the 16th of March 1974;

312   deposited as follows: UTA-A-4010, UTA-A-4021–4026, UTA-A-4036 (cleared, stained),

313   UTA-A-4031 (series of 4 juveniles); USNM197435–7; AMNH89813; UMMZ134290;

314   CM58829; UT46434.

315

316   *3.1.2.4. Material examined.* Images of the male holotype UTA-A-4011, paratypes UTA-A-

317   4010, UTA-A-4025–4026 (photos by Gregory Pandelis), AMNH89813 and USNM197435

14

318   (Fig. 3) as well as images of the following three non-type referred specimens: females

319   ANDES-A4380, 4381; male ANDES-A4382 (Appendix B)

320

321   *3.1.2.5. Definition and diagnosis.* (1) medium-sized *Synapturanus* (average male SVL 25.1

322   [23.7–26.4 mm, *n* = 12] (Pyburn, 1975); (2) head flat in lateral view; (3) eyes small, slightly

323   smaller than eye-naris distance; (4) fingertips slightly tapering; (5) subarticular tubercles

324   barely distinct on Finger III, not visible on the other fingers; (6) metacarpal tubercle large and

325   prominent; (7) Fingers II and III with a rudimentary preaxial fringe extending towards the

326   base of fingers in males and females; (8) toe tips slightly expanded on Toes III, IV and V; (9)

327   inner metatarsal tubercle small but conspicuous, outer metatarsal tubercle indistinct; (10)

328   dorsal color pattern medium brown with sparse spots (orange to gray in life, cream in

329   preservative), a discontinuous stripe extends from the snout along the canthus rostralis and

330   upper eyelid to midway between eye and axilla; (11) venter pearl white with sparse

331   melanophores, throat gray in males and females; (12) inconspicuous depressions on the

332   prootic and frontoparietal, sphenoid-nasal bridge and septum highly ossified, phalanges I–II

333   of Finger III equal to metacarpal in length, tibiale and fibulare only fused on extremities, axis

334   processes without enlarged terminals parts and atlas without a bulbous neural spine; (13) call

335   consisting in a tonal note 0.07–0.09 s in length with a slight downward frequency modulation

336   (delta 14–91 Hz) and a dominant frequency at 1.31–1.57 kHz (*n* = 6) (Table 2).

337

338   *3.1.2.6. Advertisement call.* Six males calling from underground galleries were recorded from

339   a distance of about 2 m at air temperatures ranging from 22 to 24°C (temperatures in the

340   burrows unknown). Descriptive statistics of call parameters are presented in Table 2.

341   *Synapturanus salseri* emits single tonal notes (note length mean = 0.078, range 0.071–0.090

342   s) every 5.31 s on average (range 2.36–9.16 s). The spectral structure of the note has a

343   developed harmonic structure and the dominant frequency is 1.41 kHz on average (range

344   1.31–1.57 kHz) with a slight downward modulation (ca. 0.01–0.09 kHz) (Fig. 3, Table 2).

345

346   *3.1.2.7. Remarks.* A call recorded by Pyburn from Timbo, Vaupés, Colombia, was probably

347   assigned in error to *S. salseri* by Fouquet et al. (2021) since the dominant frequency of this

348   call (1.02 kHz) does not match the values provided by Pyburn (1975) in the original

349   description (1.4 kHz). Based on the lower frequency, this call recording may in fact

350   correspond to the call of the larger species, identified as *S. mirandaribeiroi* by Pyburn (1975),

351   a species co-occurring with *S. salseri*, and possibly yet unnamed as this call does not match

352   that of *S. mirandaribeiroi* either. Additional recordings from Mitu, Vaupés, Colombia (10 km

353   from Timbo), match the sonogram (dominant frequency of 1.4 kHz) provided by Pyburn

354   (1975) and were used in the description of the advertisement call above. A recorded calling

355   specimen from Mitu (ANDES-A4382) is morphologically similar to the type specimens and

356   Pyburn's description (Fig. 3).

357

358   *3.1.2.8. Habitat and natural history.* This species occurs in pristine and secondary growth

359   *terra firme* forest. Pyburn (1975) described a clutch of four eggs and two other nests with six

360   larvae and four froglets, respectively. They were all found in underground chambers guarded

361   by a male connected to the surface by smooth walled burrows up to 15 cm deep directly

362   below the root layer. Larvae are endotrophic after hatching, which happens at least at stage 37

363   of Gosner (1960). Pyburn (1975) also reported on the stomachs of four frogs that contained 33

364   ants of the genera *Solenopsis* and *Pheidole*, and one spider.

365

16

366   *3.1.2.9. Distribution and conservation status.* The species is only known with certainty from

367   Timbo, Vaupés, Colombia, and surrounding areas (Mitu). *Synapturanus salseri* occurs at

368   about 200 m asl.

369   Given that the range of the species likely extends further, we suggest this species to be

370   considered as Data Deficient according to IUCN criteria (IUCN, 2020).

371

372   *3.1.3.1. Synapturanus zombie* sp. nov.

373   *Synapturanus mirandaribeiroi* Nelson and Lescure, 1975

374   *Synapturanus* sp. "Eastern Guianas" Vacher et al., 2020; Fouquet et al., 2021

375

376   *3.1.3.2. Holotype.* MNHN-RA-2020.0091 (field number AF3986), an adult male collected by

377   E. Courtois and M. Dewynter on the 14th of November 2018 at Itoupé, French Guiana

378   (3.0230°N 53.0955°W, ~600 m elevation; Figs. 4).

379

380   *3.1.3.3. Paratypes.* Five males: MNHN-RA-2020.0090 (AF3985), collected with the

381   holotype, MNHN-RA-2020.0088 (AF3722), MNHN-RA-2020.0089 (AF3723), collected by

382   A Fouquet, E. Courtois, B. Villette and M. Dewynter on the 16th of January 2016 at Itoupé,

383   French Guiana (3.0230°N 53.0955°W), MNHN-RA-1982.131 collected by L. Gruner on the

384   11th of November 1969 at Alikéné, French Guiana (3.2090°S 52.4020°W); MNHN-RA-

385   2020.0086 (AF1315) collected by S. Barrioz on the 6th of November 2013 at Manare, French

386   Guiana (4.1833°N 52.1500°W); and three females: MZUSP159220 (MTR24135) collected by

387   S. Marques de Souza, J. Dias Lima and A. Fouquet on the 2nd of December 2012 at Oiapoque,

388   Amapá, Brazil (3.8794°N 51.7710°W); MNHN-RA-2020.0085 (AF0525) collected by M.

389   Dewynter on the 19th of April 2008 at Saul, French Guiana (3.6376°N 53.2137°W); MNHN-

390   RA-2020.0087 (AF3573) collected by A. Fouquet, E. Courtois, B. Villette and M. Dewynter

391   on the 16th of January 2016 at Itoupé, French Guiana (3.0230°N 53.0955°W).

392

393   *3.1.3.4. Definition and diagnosis.* (1) large-sized *Synapturanus* (average male SVL 39.3 mm

394   [37.0–40.6, *n* = 4], female SVL 39.9 mm [38.7–42.1, *n* = 3]) (Table 1); (2) head dorsally

395   convex in lateral view; (3) eyes small, slightly larger than half the size of the eye-naris

396   distance; (4) fingertips tapering except on Finger IV that has a rounded tip; (5) subarticular

397   tubercles not visible on fingers; (6) thenar tubercle large and prominent, palmar tubercle

398   indistinct; (7) fingers with pre- and postaxial fringes (except postaxially on Finger IV),

399   particularly developed on Fingers II and III where fringes extend towards the base of fingers

400   in males and females; (8) toe tips expanded; (9) inner metatarsal tubercle ovoid and

401   conspicuous, outer metatarsal tubercle indistinct; (10) dorsal color pattern medium brown

402   with abundant spots and blotches over the back, head, arms and legs (orange in life, cream in

403   preservative), absence of stripe along the canthus rostralis and upper eyelid; (11) venter pearl

404   white with sparse tiny melanophores, throat similarly colored as dorsum in males and

405   females; (12) conspicuous depressions on the prootic and frontoparietal, sphenoid-nasal

406   bridge and septum highly ossified, axis processes with enlarged terminals parts and atlas with

407   a bulbous neural spine, phalanges I–II of Finger III shorter than metacarpal, tibiale and

408   fibulare only fused on extremities; (13) call consisting of a tonal note 0.147–0.167 s in length

409   with a downward frequency modulation (delta 104–194 Hz) with a dominant frequency at

410   1.06–1.19 kHz (*n* = 4) (Table 2).

411   *Synapturanus zombie* sp. nov. can be distinguished from *S. rabus* in being much larger

412   (SVL=37.0–42.1 mm in *S. zombie* sp. nov. vs. 16.2–19.0 mm in *S. rabus*); in having smaller

413   eyes (3.9% of SVL in *S. zombie,* 7.3% in *S. rabus*); fringes on Fingers II and III (absent in *S.*

414   *rabus*); a convex head in lateral view (flat in *S. rabus*); a medium brown dorsum with

18

numerous orange spots and blotches in life (vs. unspotted and uniformly dark brown in *S. rabus*); in lacking a stripe along the canthus rostralis and upper eyelid (vs. stripe present in *S. rabus*); in emitting a call consisting of longer notes (0.147–0.167 s in *S. zombie* vs. 0.039 s in *S. rabus*); and in having unfused tibiale and fibulare (vs. fused in *S. rabus*).

 Synapturanus zombie sp. nov. can be distinguished from *S. salseri* in being larger (SVL=37.0–40.6 mm in males of *S. zombie* sp. nov. vs. 23.7–26.4 mm in males of *S. salseri*); in having smaller eyes (3.9% of SVL in *S. zombie* sp. nov. vs. 5.4% in *S. salseri*); extensive fringes on Fingers II and III (vs. rudimentary fringes in *S. salseri*); a convex head in lateral view (vs. flat in *S. salseri*); a medium brown dorsum with numerous orange spots and blotches in life (vs. sparse spots in *S. salseri*); in lacking a stripe along the canthus rostralis and upper eyelid (vs. presence of a discontinuous stripe in *S. salseri*); in emitting a call consisting of longer notes (0.147–0.167 s in *S. zombie* vs. 0.079 s in *S. salseri*); and in having conspicuous depressions on the prootic and frontoparietal (vs. inconspicuous in *S. salseri*), axis processes with enlarged terminals parts (vs. not enlarged in *S. salseri*) and atlas with a bulbous neural spine (vs. not bulbous in *S. salseri*), phalanges I–II of Finger III shorter than metacarpal (vs. longer in *S. salseri*).

 Synapturanus zombie sp. nov. can be distinguished from *S. mirandaribeiroi* in being larger (SVL=37.0–40.6 mm in males of *S. zombie* vs. 26.6–30.8 mm in males of S. *mirandaribeiroi*); in having smaller eyes (3.9% of SVL in *S. zombie* sp. nov. vs. 5.2% in *S. mirandaribeiroi*); Fingers II and III tapering with well-developed fringes (vs. rudimentary fringes present and tip of these fingers rounded in *S. mirandaribeiroi*); a medium brown dorsum with numerous orange spots and blotches in life (vs. medium brown dorsum with diffuse mottled pattern in *S. mirandaribeiroi*); in lacking a stripe along the canthus rostralis and upper eyelid (vs. stripe present in *S. mirandaribeiroi*); and in emitting a call consisting of tonal notes (vs. pulsed in *S. mirandaribeiroi*).

440

3.1.3.5. Description of the holotype. An adult male, 37.0 mm SVL; body stout; head as long as wide, HL 20% of SVL; dorsal and ventral skin smooth from head to cloaca; linea masculina visible through the translucent ventral skin in life, extending ventrolaterally from axilla to groin; supratympanic fold running from the posterior corner of the eye, curving towards the axilla, continuous with an occipital (postcephalic) fold and a gular fold; presence of a thoracic fold; snout long and strongly protruding, projecting well beyond the end of the lower jaw (2.73 mm), tip rounded in dorsal and lateral view. Eyes small, 66% of EN; nares located laterally, closer to the tip of the snout (1.75 mm) than to the eye (2.27 mm); canthus rostralis rounded, loreal region strongly concave, grooved; IN 34% of HW; EN 32% of HL. Tympanum concealed and only distinct anteroventrally, obscured posterodorsally by the supratympanic fold; choanae small (50% of ED), drop shaped, located anterolaterally, no odontophore.

Forelimb robust, skin smooth; HAND 20% of SVL; Finger II longer than Finger I when fingers adpressed; fingers short, tips tapering, unwebbed, with pre- and postaxial fringes (except postaxially on Finger IV), particularly developed on Fingers II and III where fringes extend towards the base of fingers; no finger discs; relative length of adpressed fingers III > IV > II > I; subarticular tubercles not visible on fingers; thenar tubercle large and prominent, palmar tubercle indistinct. Glandular unpigmented supracarpal pad.

Hind limb robust, skin smooth; TL 35% of SVL; FL 37% of SVL; relative length of adpressed toes IV > III > V > II > I; Toe I very short, its tip reaching the base of Toe II when toes adpressed; toes without discs, tips as large as width of toes. Toes unwebbed with narrow pre- and postaxial fringes. Subarticular tubercles not visible on toes; inner metatarsal tubercle ovoid, large (1.2 mm) and prominent, outer metatarsal tubercle indistinct. Metatarsal fold absent.

465

466 *3.1.3.6. Color of holotype in life.* Dorsal color medium brown with numerous orange spots

467 and blotches over the back, head, arms and legs. Flanks light brown with abundant orange

468 spots and blotches. Absence of a stripe along the canthus rostralis and upper eyelid, but a few

469 aligned spots form a discontinuous series. Snout white, unpigmented. Throat medium brown

470 with orange spots; belly translucent pearl white with small melanophores (Fig. 4). Upper and

471 lower arm and dorsal surfaces of thigh, shank and tarsus similar to the dorsum in color.

472 Glandular supracarpal pad translucent white.

473

474 *3.1.3.7. Color of holotype in preservative*. After four years in 70% ethanol, colors of the

475 specimen faded with the orange spots and blotches turning white as well as the glandular

476 supracarpal pad (Fig. 4).

477

478 *3.1.3.8. Variation*. For morphometric variation see Table 1. Sexual dimorphism consists of the

479 presence of a supracarpal pad in males, and differences in body size, although males and

480 females overlap in SVL and this sexual dimorphism remains subtle. Linea masculina visible

481 in life through the translucent ventral skin in males. Yellow ovaries are visible in life through

482 the translucent skin in females, and in preservative in females. Coloration varies little across

483 specimens examined (Fig. 5), ground dorsal coloration varies from light to medium brown

484 with orange or yellowish spots in life.

485

486 *3.1.3.9. Advertisement call.* Four specimens calling from underground galleries were recorded

487 from a distance of about 2 m at air temperatures ranging from 22 to 24°C (temperatures

488 unknown inside the galleries). Descriptive statistics of call parameters are presented in Table

489 2. *Synapturanus zombie* sp. nov. emits single tonal notes (note length mean = 0.154, range

490   0.147–0.167 s) every 8.47 s on average (range 8.20–9.90 s). The spectral structure of the note

491   has a developed harmonic structure and the dominant frequency is 1.11 kHz on average

492   (range 1.06–1.19 kHz) with a strong downward modulation (ca. 0.1–0.2 kHz) (Fig. 4, Table

493   2).

494

495   *3.1.3.10. Habitat and natural history. Synapturanus zombie* sp. nov. has been found in well-

496   drained *terra firme* soils, in primary forest on the slopes of massifs and sandy soils near

497   inselbergs. They dig galleries from which the males call, spaced a few meters apart from each

498   other, during and after heavy rain showers during the weeks preceding the rainy season

499   (October-November). Females probably use the same galleries since they have been found

500   while searching for the provenance of a call. We assume that the mode of reproduction of this

501   species is similar to that of the related species for which it is documented, although this needs

502   to be confirmed by field observations.

503

504   *3.1.3.11. Etymology.* The specific epithet is a noun in apposition referring to zombies,

505   fictional undead corporeal revenants, originating from Haitian folklore and omnipresent in

506   pop culture movies. The call of this species is only heard during and after heavy rain showers,

507   when herpetologists are often not properly equipped, thus ending up soaked and digging with

508   their bare hands in the mud in the midst of thunderstorms, reminiscent of zombies extracting

509   themselves from the ground.

510

511   *3.1.3.12. Distribution and conservation status. Synapturanus zombie* sp. nov. is only known

512   from six groups of populations in French Guiana (Savane Virginie/Mataroni, Trois Pitons,

513   Saut Maripa, Alikéné, Saul, Itoupé, Mont Chauve) and one population in Amapá, Brazil

514   (Oiapoque) (Fig. 2). An additional likely locality in Amapá is "Rivière Lunier" (Upper Rio

515 Calçoene=Haut-Carsevenne) (2.3734°N, 51.3782°W) but it corresponds to a lost specimen

516 from MNHN (J. Lescure, pers. comm.). This species is most likely endemic to the

517 easternmost part of the Guiana Shield. In French Guiana, *S. mirandaribeiroi* is found in the

518 southwestern corner of the territory and the species do not seem to co-occur, suggesting a

519 boundary in their respective distributions and possibly exclusion. *Synapturanus zombie* sp.

520 nov. is absent from the northwestern part of French Guiana with a putative limit at the level of

521 the Approuague basin, a distribution pattern similar to that of several other species such as

522 *Amazophrynella teko* Rojas-Zamora, Fouquet, Ron, Hernández-Ruz, Melo-Sampaio,

523 Chaparro, Vogt, Carvalho, Pinheiro, Ávila, Farias, Gordo, and Hrbek, 2018; *Leptodactylus*

524 *longirostris* (Boulenger, 1882) or *Pristimantis* sp. (= *P*. sp. 1 of Fouquet et al., 2013).

525 *Synapturanus zombie* sp. nov. is found between 100–600 m asl. Its range is most likely small

526 and the populations seem isolated from each other, but it is such a difficult species to detect

527 that this remains speculative.

528   Given the uncertainties regarding its distribution and population status, we suggest

529 considering the species as Data Deficient according to IUCN criteria (IUCN, 2020). Some of

530 the known populations occur in protected areas in French Guiana (i.e., in the Parc Amazonien

531 de Guyane).

532

533 *3.1.4.1. Synapturanus mesomorphus* sp. nov.

534 *Synapturanus mirandaribeiroi* Nelson and Lescure, 1975; Ernst et al., 2005

535 *Synapturanus salseri* Kok and Kalamandeen, 2008; Cole et al., 2013

536 *Synapturanus* sp. "Guyana" Vacher et al., 2020; Fouquet et al., 2021

537

3.1.4.2. Holotype. MTD48012 (field number RE-040), an adult female, collected by Monique

Hölting and Raffael Ernst the 21st of May 2010 at Iwokrama, Guyana (4.6713°N, 58.7751°W,

~160 m elevation; Figs. 6,7).

3.1.4.3. Paratypes. Six males: AMNH166450 (JC7727), collected by C.J. Cole and C.R.

Townsend between the 3rd and 6th of March 1998 in Magdalen's Creek camp, near (275 m)

NW bank of the Konawaruk River, Guyana (5.2186°N 59.0453°W); SMNS12077–78

(MABM0202, MABM0102) collected by R. Ernst on the 16th and the 14th of November 2002,

respectively, in Mabura Hill Forest Reserve, Guyana (5.1553°N 58.6997°W); RBINS4202

(PK1397), collected by P.J.R. Kok, P. Benjamin and G. Seegobin on the 28th of March 2006

in Kaieteur National Park, Guyana (5.1333°N 59.4167° W); RBINS4204 (PK1577), collected

by P.J.R. Kok, P. Benjamin and G. Seegobin on the 26th of June 2006 in Kaieteur National

Park, Guyana (5.1333°N 59.4000° W); USNM588794 (BPN3813), collected by A. Snyder on

the 5th of March 2014 at Bay Camp, Potaro-Siparuni, Guyana (5.0115°N 59.6431°W). Seven

females: USNM566235 (JC7845), by C.J. Cole and C.R. Townsend between the 10 and 11th

of March 1998 in Magdalen's Creek camp, near (275 m) NW bank of the Konawaruk River,

Guyana (5.2186°N 59.0453°W); RBINS4201 (PK1396), collected by P.J.R. Kok, P.

Benjamin and G. Seegobin on the 28th of March 2006 in Kaieteur National Park, Guyana

(5.1333°N 59.4167°W); RBINS4205 (PK1641), collected by G. Seegobin in November 2006

in Kaieteur National Park, Guyana (5.1333°N 59.4167°W); RBINS4206–07 (PK1137,

PK1143), collected by F. Marco in January 2006 in Kaieteur National Park, Guyana

(5.1969°N 59.4817°W); USNM588793 (BPN3762), collected by A. Snyder on the 11th of

March 2014 at Bay Camp, Potaro-Siparuni, Guyana (5.0115°N 59.6431°W); MTD49061

(RE-MH27), collected by M. Hölting and R. Ernst on the 23rd of June 2014 in Iwokrama

Forest Reserve, Guyana (4.4942°N, 58.7759°W). One juvenile: RBINS4203 (PK1570),

563 collected by P.J.R. Kok, P. Benjamin and G. Seegobin on the 23rd of June 2006 in Kaieteur

564 National Park, Guyana (5.1333°N 59.4167° W).

565

566 *3.1.4.4. Material examined.* We additionally examined 10 referred specimens (see Appendix

567 B).

568

569 *3.1.4.5. Definition and diagnosis.* (1) medium-sized *Synapturanus* (average male SVL 24.7

570 mm [22.9–26.0, $n = 6$], female SVL 27.9 mm [26.3–29.4, $n = 11$]) (Table 1); (2) head convex

571 in lateral view; (3) eyes small, slightly smaller than eye-naris distance; (4) fingertips rounded;

572 (5) subarticular tubercles not visible on fingers; (6) thenar tubercle barely distinct, palmar

573 tubercle indistinct; (7) Fingers II and III with preaxial fringes in males and females, extending

574 towards the base of fingers; (8) toe tips expanded; (9) inner metatarsal tubercle small, ovoid,

575 outer metatarsal tubercle indistinct; (10) dorsal color pattern dark to light brown with sparse

576 small speckles and blotches over the back, head, arms and legs (beige in life, cream in

577 preservative), a more or less continuous stripe (often broken in small flecks/spots) extends

578 from the snout along the canthus rostralis and upper eyelid to midway between eye and axilla;

579 (11) venter pearl white with melanophores, throat color similar to dorsal color in males and

580 females; (12) inconspicuous depressions on the prootic and frontoparietal, sphenoid-nasal

581 bridge and septum highly ossified, axis processes with enlarged terminals parts and atlas large

582 with an inconspicuous bulbous neural spine, phalanges I–II of Finger III equal to metacarpa in

583 length, tibiale and fibulare only fused on extremities; (13) call consisting in a tonal note

584 0.160–0.173 s in length with a dominant frequency at 1.06–1.13 kHz ($n = 2$) (Fig. 6, Table 2).

585   *Synapturanus mesomorphus* sp. nov. can be distinguished from *S. rabus* in being

586 larger (SVL=22.9–29.4 mm in *S. mesomorphus* sp. nov. vs. 16.2–19.0 mm in *S. rabus*); in

587 having smaller eyes (5.1% of SVL in *S. mesomorphus* sp. nov. vs. 7.3% in *S. rabus*); preaxial

588 fringes on Fingers II and III (vs. no fringes in *S. rabus*); a convex head in lateral view (vs. flat

589 in *S. rabus*); a brown dorsum with sparse speckles and beige blotches in life (vs. dorsum

590 uniformly brown in *S. rabus*); a call consisting of longer notes (0.160–0.173 s in *S.*

591 *mesomorphus* sp. nov. vs. 0.039 in *S. rabus*); and tibiale and fibulare only fused on

592 extremities (vs. entirely fused in *S. rabus*).

593   *Synapturanus mesomorphus* sp. nov. is most similar to *S. salseri*, from which it can be

594 distinguished by having a convex head in lateral view (flat in *S. salseri*); a call consisting of

595 longer notes (0.160–0.173 s in *S. mesomorphus* sp. nov. vs. 0.079 in *S. salseri*); and axis

596 processes with enlarged terminal parts (vs. not enlarged in *S. salseri*) and atlas with a bulbous

597 neural spine (vs. not bulbous in *S. salseri*).

598   *Synapturanus mesomorphus* sp. nov. can be distinguished from *S. mirandaribeiroi* in

599 having a smaller body size (SVL=22.9–26.0 mm in males of *S. mesomorphus* vs. 26.6–30.8

600 mm in males of *S. mirandaribeiroi*); a brown dorsal coloration with sparse speckles and

601 blotches (diffuse mottled pattern in *S. mirandaribeiroi*); a call consisting of tonal notes (vs.

602 pulsed in *S. mirandaribeiroi*); and inconspicuous depressions on the prootic and frontoparietal

603 (vs. conspicuous in *S. mirandaribeiroi*), phalanges I–II of Finger III equal to metacarpa in

604 length (vs. shorter in *S. mirandaribeiroi*).

605   *Synapturanus mesomorphus* sp. nov. can be distinguished from *Synapturanus zombie*

606 sp. nov. in being smaller (SVL=22.9–26.0 mm in males of *S. mesomorphus* vs. 37.0–40.6 mm

607 in males of *S. zombie* sp. nov.); in having a light to dark brown dorsal coloration with sparse

608 beige speckles and blotches (vs. medium brown with numerous orange spots and blotches in

609 *S. zombie*); a stripe running along the canthus rostralis and the upper eyelid to midway

610 between eye and axilla (vs. stripe absent in *S. zombie* sp. nov.); a call lacking downward

611 frequency modulation (vs. 104–194 Hz decrease in *S. zombie* sp. nov.); and inconspicuous

612 depressions on the prootic and frontoparietal (vs. conspicuous in *S. zombie* sp. nov.),

613 phalanges I–II of Finger III equal to metacarpals in length (vs. shorter in *S. zombie* sp. nov.).

614

615 *3.1.4.6. Description of the holotype.* (Fig. 6) An adult female, 29.4 mm SVL; body stout; head

616 slightly wider than long, HL 20% of SVL; dorsal and ventral skin smooth; supratympanic fold

617 running from the posterior corner of the eye, curving towards the axilla, continuous with an

618 occipital (postcephalic) fold and a gular fold; presence of a thoracic fold; snout long and

619 strongly protruding, projecting well beyond the end of the lower jaw (2.0 mm), rounded in

620 dorsal and lateral view. Eyes small, 85% of EN; nares located laterally closer to the tip of the

621 snout (1.03 mm) than to the eye (1.91 mm); canthus rostralis rounded, loreal region strongly

622 concave with a groove between the naris and the eye; IN 29% of HW; EN 32% of HL.

623 Tympanum concealed and only distinct anteroventrally, obscured posterodorsally by a

624 supratympanic fold; choanae small (50% of ED), drop shaped, located anterolaterally, no

625 odontophore.

626 Forelimb robust, skin smooth; HAND 16% of SVL; Finger II longer than Finger I

627 when fingers adpressed; fingers short with rounded tips, unwebbed, with preaxial fringes on

628 Fingers II and III extending towards the base of fingers; no finger discs; relative lengths of

629 adpressed fingers III > IV > II > I; subarticular tubercles not visible on fingers; thenar

630 tubercle large and prominent, palmar tubercle indistinct.

631 Hind limb robust, skin smooth; TL 40% of SVL; FL 38% of SVL; relative length of

632 adpressed toes IV > III > V > II > I; Toe I very short, its tip reaching the base of Toe II when

633 toes adpressed; toe without discs; Toes II, III, IV and V have expanded tips. Toes unwebbed;

634 narrow preaxial fringes on Toes II–V and postaxial fringes on Toes II–IV; subarticular

635 tubercles not visible on toes; inner metatarsal tubercle ovoid (0.85 mm); outer metatarsal

636 tubercle indistinct; metatarsal fold absent.

637

638 *3.1.4.7. Color of holotype in life.* Dorsal color light brown with few, very small beige speckles

639 over the back and head, more abundant on arms and legs. Flanks light grayish brown with

640 larger and more abundant beige blotches. More or less continuous stripe along the canthus

641 rostralis and upper eyelid, formed by aligned speckles. Snout gray. Throat light brown,

642 immaculate; belly translucent gray with small melanophores (Fig. 7). Upper and lower arm

643 and dorsal surfaces of thigh, shank and tarsus similar to the flanks in color.

644

645 *3.1.4.8. Color of holotype in preservative.* After ten years in 70% ethanol, colors of the

646 specimen generally faded (Fig. 6).

647

648 *3.1.4.9. Variation.* For morphometric variation see Table 1. Sexual dimorphism is apparent in

649 size (SVL of males and females do not overlap) and in the presence of a supracarpal pad in

650 males (poorly visible in preservative). Ovaries are visible through the translucent skin in

651 gravid females. Background coloration varies extensively across specimens from light brown

652 to dark brown. Spot color varies from white, beige to orange. The stripe along the canthus

653 rostralis and upper eyelid can be markedly discontinuous (as in the holotype), or extending

654 only a few mm posteriorly to the eye (RBINS15789) to as long as extending to the axilla

655 (RBINS15790) (Fig. 7). This stripe can either be narrow or relatively broad, notably along the

656 canthus rostralis (RBINS15789).

657

658 *3.1.4.10. Advertisement call.* Two specimens calling from underground galleries were

659 recorded from a distance of about 2 m at air temperatures ranging from 22 to 25°C

660 (temperatures in the galleries unknown). Descriptive statistics of call parameters are presented

661 in Table 2. *Synapturanus mesomorphus* sp. nov. emits single tonal notes (note length mean =

662 0.166, range 0.160–0.173 s) every 10.29 s on average (range 9.66–10.93 s). The spectral

663 structure of the note has a developed harmonic structure and the fundamental (dominant

664 frequency) is 1.09 kHz on average (range 1.06–1.13 kHz) with a slight downward modulation

665 between the beginning and the end of the note (ca. 0.01–0.04 kHz) (Fig. 6, Table 2).

666

667 *3.1.4.11. Habitat and natural history.* The habitats where *Synapturanus mesomorphus* sp.

668 nov. was found range from clearings in white sand forest to well-drained mixed forest on

669 white sand and brown sand (ferralic arenosols) in the vicinity of riverine floodplain forest on

670 alluvial soils, but always in un-inundated areas. Males call from burrows in the ground, below

671 the leaf litter and exclusively during drizzling or heavy rainfalls. Calling activity seems

672 triggered by the sound of the rain drops on the ground. Most of our specimens were collected

673 in the early morning in pitfall traps, indicating active movements above the ground at night,

674 or were actively excavated from small burrows while calling, during or shortly after rainfall.

675 One uncatalogued specimen (PK3789) was found active on the ground at dusk. Reproduction

676 and clutches have never been directly observed. However, we assume that eggs are laid in

677 burrows below the soil surface and that tadpoles do not feed and complete their development

678 within the burrow as in other related species. Nelson and Lescure (1975) reported on the

679 stomach content of a specimen from Demerara Falls containing only ants, which is consistent

680 with the gut contents of one dissected specimen (RBINS15789). However, the stomachs of

681 some other specimens that were dissected (e.g., paratype RBINS4202 and RBINS15812)

682 contained a large number of termites, including large soldiers. In Mabura Hill, no record of

683 calling activity was made outside a very short reproductive period, which was restricted to

684 only a very few nights annually (Ernst et al., 2005).

685

686 *3.1.4.12. Etymology.* The specific epithet comes from the Greek *mesos* (middle, intermediate)

687 and *morphē* (sort, appearance, form) and refers to the intermediate morphology of the species

688 between the easternmost species of the eastern clade and the species of the western clade

689 (Fouquet et al., 2021).

690

691 *3.1.4.13. Distribution and conservation status.* This species is currently known from eight

692 localities in Guyana (Mabura Hill Forest Reserve, Iwokrama Forest Reserve, Kaieteur

693 National Park, Bay Camp, Meamu River, Kuribrong, Konawaruk Camp, Kartabo) on the

694 eastern edge of Pantepui, or at the boundaries between Pantepui and the lowlands of the

695 Eastern Guiana Shield (Fig. 2). *Synapturanus mesomorphus* sp. nov. might occur in

696 neighboring Venezuela (La Escalera, Sierra de Lema 6.6670°N 62.4170°W - Barrio-Amorós

697 et al. 2011; Cerro Santa Rosa Serrania del Supamo 6.6170°N 62.4500°W; Barrio-Amorós and

698 Brewer-Carías, 1999) and in the southern part of Guyana where it could enter in contact with

699 *S. mirandaribeiroi. Synapturanus mesomorphus* sp. nov. is found between 100–580 m asl. It

700 is unlikely that this species extends much further than its small currently recognized range.

701 The area where this species occurs is heavily impacted by past and ongoing gold-mining

702 activities (Dezecache et al., 2017). Although some of the known populations are within

703 protected areas (Iwokrama, Kaieteur, Mabura) a significant portion of the range of the species

704 is threatened by illegal activities, such as the aforementioned mining and rampant

705 deforestation (Ernst et al., 2006).

706   Considering the small number of known populations (<10), the small range (<20,000

707 km2) and their likely decline in the upcoming future we suggest that *Synapturanus*

708 *mesomorphus* sp. nov. should be considered as Vulnerable (B1ab(iii)) by the IUCN.

709

710 *3.1.5.1. Synapturanus ajuricaba* sp. nov.

711 *Synapturanus mirandaribeiroi* Nelson and Lescure, 1975

712 *Synapturanus salseri* Lima et al., 2006; Peloso et al., 2014

713 *Synapturanus* cf. *salseri* Menin et al., 2007

714 *Synapturanus* sp. "Manaus" Vacher et al., 2020; Fouquet et al., 2021

715

716 *3.1.5.2. Holotype.* INPA-H38464 (field n°CTGA-1804), an adult female, collected by A.

717 Almeida, R.R. Rojas, A. Oliveira and O. Pereira on the 1st of December 2013 on the right

718 bank of Trombetas River, Pará, Brazil (1.3818°S 56.8630°W, ~100 m elevation; Fig. 8).

719

720 *3.1.5.3. Paratypes.* Five males: MPEG29453 (CN370), MPEG29454 (CN373), MPEG29456

721 (CN416), MPEG29457 (CN523), MPEG29458 (CN590) collected by M.S. Hoogmoed and

722 W. Rocha between the 16th and the 26th of April 2008 at Floresta Estadual de Trombetas,

723 Pará, Brazil (0.9628°S 55.5223°W); and two females: INPA-H28519 collected by V.T. de

724 Carvalho on the 1st of September 2007 at Sítio Renato Cintra, Ponte Cacau Pereira,

725 Amazonas, Brazil (3.1050°S 60.0691°W); and INPA-H35751 collected by A.F. Palmeirim on

726 the 13th of June 2015 at Ilha Sapupara, Amazonas state, Brazil (1.8924°S 59.4487°W).

727

728 *3.1.5.4. Diagnosis and comparisons.* (1) medium-sized *Synapturanus* (average male SVL 31.8

729 mm [29.3–33.2, *n* = 5], female SVL 36.5 mm [35.9–37.3, *n* = 3]) (Table 1); (2) head dorsally

730 convex in lateral view; (7) tympanum concealed and only distinct anteroventrally; (3) eyes

731 small, almost half the size of the eye-naris distance; (4) fingertips tapering, except on Finger

732 IV that has a rounded tip; (5) subarticular tubercles not visible on fingers; (6) thenar tubercle

733 large and prominent, palmar tubercle indistinct; (7) Fingers II and III with well-developed

734 preaxial fringe extending towards the base of fingers, and Fingers I and II with narrow

735 postaxial fringe in males and females; (8) toe tips slightly expanded; (9) inner and outer

metatarsal tubercles indistinct; (10) dorsal color pattern medium brown with numerous small spots (orange in life, cream in preservative) forming a mottled pattern over the back and head with spots increasing in size towards the flanks, arms and legs, a more or less continuous stripe (often broken in small fleck/spots) extends from the snout along the canthus rostralis and upper eyelid to midway between eye and axilla; (11) venter pearl white with sparse melanophores, throat similarly colored as dorsum in males and females; (12) conspicuous depressions on the prootic and frontoparietal, sphenoid-nasal bridge and septum highly ossified, axis processes with enlarged terminals parts and atlas with a bulbous neural spine, phalanges I and II of Finger III shorter than metacarpal, tibiale and fibulare only fused on extremities; (13) call consisting in a pulsed note 0.282–0.366 s in length with a dominant frequency at 1.01–1.12 kHz ($n = 5$) (Fig. 8, Table 2).

Synapturanus ajuricaba sp. nov. can be distinguished from *S. rabus* by considerably being larger (SVL=29.3–37.3 mm in *S. ajuricaba* vs. 16.2–19.0 mm in *S. rabus*); in having smaller eyes (4.9% of SVL in *S. ajuricaba* vs. 7.3% in *S. rabus*); well-developed fringes on Fingers II and III (vs. no fringes in *S. rabus*); a convex head in lateral view (vs. flat in *S. rabus*); a brown dorsum with a mottled pattern (vs. uniformly dark brown in *S. rabus*); a call consisting of longer and pulsed notes (0.282–0.366 s in *S. ajuricaba* vs. 0.039 and tonal in *S. rabus*); and conspicuous depressions on the prootic and frontoparietal (inconspicuous in *S. rabus*) and tibiale and fibulare only fused on extremities (totally fused in *S. rabus*).

Synapturanus ajuricaba sp. nov. can be distinguished from *S. salseri* in being larger (SVL=29.3–33.2 mm in males of *S. ajuricaba* vs. 23.7–26.4 mm in males of *S. salseri*); in having smaller eyes (4.9% of SVL in *S. ajuricaba* vs. 5.4% in *S. salseri*); well-developed fringes on Fingers II and III (vs. rudimentary fringes in *S. salseri*); a convex head in lateral view (vs. flat in *S. salseri*); a brown dorsum with a mottled pattern (vs. sparse spots in *S. salseri*); a call consisting of longer and pulsed notes (0.282–0.366 s in *S. ajuricaba* vs. 0.079

761   and tonal in *S. salseri*); and conspicuous depressions on the prootic and frontoparietal

762   (inconspicuous in *S. salseri*), axis processes with enlarged terminals parts (vs. not enlarged in

763   *S. salseri*) and atlas with a bulbous neural spine (vs. not bulbous in *S. salseri*), phalanges I and

764   II of Finger III shorter than metacarpal (vs. longer in *S. salseri*).

765   *Synapturanus ajuricaba* sp. nov. can be distinguished from *S. mirandaribeiroi* in

766   having Fingers II and III tapering with well-developed fringes (vs. fingertips rounded and less

767   developed fringes in *S. mirandaribeiroi*); and a call consisting of longer notes with partly

768   fused pulses (0.282–0.366 s and 12–16 partly fused pulses vs. 0.130–0.194 s and 5–8 entirely

769   fused pulses in *S. mirandaribeiroi*).

770   *Synapturanus ajuricaba* sp. nov. can be distinguished from *S. zombie* sp. nov. in being

771   smaller (SVL=29.3–33.2 mm in males of *S. ajuricaba* sp. nov. vs. 37.0–40.6 mm in males of

772   *S. zombie* sp. nov.); in having a stripe along the canthus rostralis and upper eyelid extending

773   between eye and axilla (stripe absent in *S. zombie* sp. nov.); and in having a call consisting of

774   longer pulsed notes (0.282–0.366 s and 12–16 partly fused pulses vs. 0.147–0.167 s and tonal

775   notes in *S. zombie*).

776   *Synapturanus ajuricaba* sp. nov. can be distinguished from *S. mesomorphus* sp. nov.

777   by being larger (SVL=29.3–33.2 mm in males of *S. ajuricaba* sp. nov. vs. 22.9–26.0 mm in

778   males of *S. mesomorphus* sp. nov.); in having a brown dorsum with a mottled pattern (vs.

779   light to dark brown with sparse speckles and blotches in *S. mesomorphus* sp. nov.); a call

780   consisting of longer pulsed notes, with 0.282–0.366 s and 12–16 partly fused pulses (0.160–

781   0.173 s and tonal notes in *S. mesomorphus*); and conspicuous depressions on the prootic and

782   frontoparietal (vs. inconspicuous in *S. mesomorphus*), phalanges I and II of Finger III shorter

783   than metacarpal (vs. same size in *S. mesomorphus*) .

784

785 *3.1.5.5. Description of the holotype.* An adult female, 35.9 mm SVL; body stout; head slightly

786 longer than wide, HL 18% of SVL; dorsal and ventral skin smooth; supratympanic fold

787 running from the posterior corner of the eye, curving towards the axilla, continuous with an

788 occipital (postcephalic) fold and a gular fold; presence of a thoracic fold; snout long and

789 strongly protruding, projecting well beyond the end of the lower jaw (1.94 mm), rounded in

790 dorsal and lateral view. Eyes small, 64% of EN; nares located laterally closer to the tip of the

791 snout (1.3 mm) than to the eye (2.5 mm); canthus rostralis rounded, loreal region strongly

792 concave, grooved; IN 34% of HW; EN 39% of HL. Tympanum concealed and only distinct

793 anteroventrally, obscured posterodorsally by a supratympanic fold; choanae small (50% of

794 ED), drop shaped, located anterolaterally, no odontophore.

795 Forelimb robust, skin smooth; HAND 16% of SVL; Finger II longer than Finger I

796 when fingers adpressed; fingers short, tips tapering, except on Finger IV that has a rounded

797 tip, unwebbed, with pre- and postaxial fringes (except postaxially on Finger IV), particularly

798 developed on Fingers II and III and extending towards the base of fingers; no finger discs;

799 relative lengths of adpressed fingers III > IV > II > I; subarticular tubercles not visible on

800 fingers; thenar tubercle large and prominent, palmar tubercle indistinct.

801 Hind limb robust, skin smooth; TL 35% of SVL; FL34% of SVL; relative length of

802 adpressed toes IV > III > V > II > I; Toe I very short, its tip reaching the base of Toe II when

803 toes adpressed; toe without discs, Toes II, III and IV have slightly expanded tips. Toes

804 unwebbed with narrow pre- and postaxial fringes. Subarticular tubercles not visible on toes;

805 inner and outer metatarsal tubercle indistinct. Metatarsal fold absent.

806

807 *3.1.5.6. Color of holotype in life.* Information not available.

808

34

3.1.5.7. Color of holotype in preservative. Dorsum medium brown with numerous small cream spots forming a mottled pattern over the back and head with spots increasing in size towards the flanks, arms and legs, presence of a stripe along the canthus rostralis and upper eyelid that extends midway between eye and axilla. Venter pearl white with sparse melanophores, throat similar to the dorsum in color (Fig. 8).

3.1.5.8. Variation. For morphometric variation see Table 1. Sexual dimorphism is apparent in the presence of a supracarpal pad in males, but dimorphism in body size remains subtle. Linea masculina visible in life through the translucent ventral skin in males. Ovaries are visible through the translucent skin in gravid females, and in preservative in females. Coloration varies little across specimens (Fig. 9).

3.1.5.9. Advertisement call. Five specimens calling from underground galleries were recorded from a distance of about 2 m at air temperatures ranging from 22 to 24°C (temperatures unknown in galleries). Descriptive statistics of call parameters are presented in Table 2. *Synapturanus ajuricaba* sp. nov. emits single pulsed notes (note length mean = 0.322, range 0.282–0.366 s) every 6.91 s on average (range 5.2–9.04 s). The spectral structure of the note has a developed harmonic structure and the fundamental (dominant frequency) is 1.06 kHz on average (range 1.01–1.12 kHz). These notes are composed of 12–16 partly fused pulses (ca. 0.02 s in length) of decreasing energy and with a downward frequency between the beginning and the end of the note (ca. 0.05–0.09 kHz) (Fig. 8, Table 2).

3.1.5.10. Habitat and natural history. This species occurs in pristine *terra firme* forest. Calling activity is mostly circumscribed during and after rain showers of November and December (Menin et al., 2008). Menin et al. (2007) provided detailed information about the

834 reproduction and embryonic/larval development of this species from a population nearby

835 Manaus, Brazil (under the name *Synapturanus* cf. *salseri*). Five clutches contained a mean of

836 eight eggs; tadpoles hatched approximately at stage 42 of Gosner (1960). All clutches were

837 found in burrows, approximately 5–10 cm below the soil surface and within 20 cm of an adult

838 male (Menin et al., 2007). Pyburn (1975) found a downward curve at the end of the tail in *S.*

839 *salseri* in stage 41. This characteristic was not observed in *S. ajuricaba* sp. nov. Moreover, the

840 total length of *S. salseri* tadpoles at stage 41 from Colombia was much greater (23.7 mm, one

841 individual) than that observed by Menin et al. (2007) in *S. ajuricaba* sp. nov. (12.6±0.6 mm,

842 n=7). Vocalizations are commonly heard during the rainy season between November and May

843 (Menin et al., 2008). We also report the presence of three ants in the stomach of one specimen

844 (INPA-H11873 from Reserva Florestal Adolpho Ducke, Manaus, Amazonas state).

845

846 *3.1.5.11. Etymology.* The specific name *ajuricaba* is used as a noun in apposition and is given

847 as a reference to the legendary indigenous figure, Ajuricaba, a prominent leader of the

848 Manaós indigenous people—considered extinct. They were one of the most important tribes

849 of the Rio Negro. Ajuricaba led several incursions by the Manaós and allied groups against

850 European settlements in the Rio Negro region. For his effort and leadership, he became one of

851 the symbols of indigenous resistance against European colonization. Ajuricaba was eventually

852 captured and was to be conducted to Belém, probably to be enslaved. History tells that during

853 his transport to the capital, while still in chains, Ajuricaba and his men rebelled against

854 captors, killing several of them. Eventually losing the battle, the survivors, including

855 Ajuricaba, jumped into the waters of the Amazon river and were never seen again. For

856 additional details about this important indigenous figure, see Souza (2019).

857

858 *3.1.5.12. Distribution and conservation status.* This species is known from five localities (Ilha

859 Sapupara, Trombetas, Floresta Nacional de Faro, Reserva Florestal Adolpho Ducke, Ponte

860 Cacau Pereira) in the northern parts of the Amazonas and the Pará states, Brazil (Fig. 2).

861 These populations range between 100 and 200 m asl.

862   We suggest considering this species as Data Deficient according to the IUCN criteria

863 (IUCN, 2020).

864

865 *3.2. Comparative osteology of Synapturanus*

866

867 *3.2.1. Ossification and preservation artefacts.* Analyses of µCT-scans revealed a conspicuous

868 variation in osteological characters within *Synapturanus.* We evaluated whether differences in

869 ossification were consistent and inherent to each species or merely due to preservation

870 artefacts by examining several adult specimens per species. Juvenile specimens were all

871 poorly ossified and therefore not used in the comparative analyses.

872   Although species in the genus can be overall considered hyperossified, some regions

873 display variable degrees of ossification, partly due to (1) interspecific variation, (2)

874 ontogenetic variation, and (3) preservation (e.g., decalcification after decades of preservation

875 in alcohol and/or use of high formalin concentration for fixation). For example, cranial bones

876 are generally fused forming a robust skull. However, the degree of fusion is variable as seen

877 through suture lines that can be completely invisible in recently collected *Synapturanus*

878 *mirandaribeiroi* (Fig. 10, MNHN-RA-2020.0084), visible as narrow grooves in *S.* sp.

879 "Ecuador" (Fig. 10; Fig. S2) or clearly differentiated in the old paratype of *S. mirandaribeiroi*

880 (Fig. 10, MNHN-RA-1974.0397). Other naturally less calcified bones, apparently prone to be

881 affected by long-term preservation, are the lateral part of the prootic and the palatine region,

882 which was previously mentioned as displaying variable ossification (Zweifel, 1986), the

883   autopod, the neural spine and the ischium (urostyle). The paratype of *S. mirandaribeiroi*

884   (MNHN-RA-1974.0397) is notably decalcified, likely because of its long-term preservation,

885   and some characters like the sphenoid-nasal bridge are impossible to evaluate (Fig. 10; Fig.

886   S2); the scapula and coracoid are differentiated while those bones are fused in other

887   specimens; the proximal epiphysis of the humerus, femur, tibio-fibula and tarsum are not

888   visible; metacarpal bone and prepollex are not visible either. The paratype of *S. salseri* is also

889   slightly decalcified, e.g., the distal epiphysis of the femur and some metacarpal bones are not

890   visible. One needs therefore to be careful when assessing the diagnostic value of these

891   characters.

892

893   *3.2.2. Cranium.* Skull robust and compact, convex in lateral view, projecting anteriorly,

894   truncate or acuminate in dorsal view, slightly longer than wide. Most cranial bones are in

895   contact but the degree of contact differs among specimens and can be categorized into three

896   states, as suggested in Kok et al. (2020): (1) free, with no contact between structures (e.g., *S.*

897   *mirandaribeiroi* MNHN-RA-1974.0397); (2) structures in contact with a visible suture line

898   (e.g., *S.* sp. "Ecuador"); or (3) fused, structures in contact with a suture line being barely

899   visible or absent (e.g., *S. zombie*) (Fig. 10). Nasal, sphenethmoid and frontoparietal are fused.

900   The posterior end of the nasal is projecting laterally well beyond the anterior end of the

901   frontoparietal, which is particularly visible when cranial bones are free (1) or with a visible

902   suture line (2). Each nasal bone generally anteriorly perforated by a nasal foramen (often

903   opening into the nasal cavity via a small canal). When present on both bones they are

904   generally positioned asymmetrically (Fig. 10; Fig. S2). These foramina are highly variable

905   among specimens and seem little informative to diagnose species. Nasal septum is dense

906   enough to be visible. The nasal extends anteriorly, curving towards the sphenethmoid forming

907   a strong arch protecting the nasal cavity. Partly calcified tissue is attached to the nasal as a

908   protruding snout extending well beyond the lower jaw. The ontology of this nasal-

909   sphenethmoid bridge is unclear and could either result from the extension of the sphenoid as

910   suggested by Nelson and Lescure (1975) or/and chondrosis of the nasal region tissue. The

911   *pars facialis* and lateral part of the nasal are not in contact.

912   The prootic region is well developed laterally, and is well ossified in all our

913   specimens. Dorsal parts of the frontal and the prootic are sculpted with two shallow

914   depressions each: at the level of the prootic/frontoparietal and in a medial position on the

915   frontal, and laterally and medially on the prootic (Fig. 10; Fig. S2). Occipital condyles are

916   ovoid and vertical. Prootic, sphenethmoid and exoccipital are ventrally fused to the

917   parasphenoid, the degree of visibility of the suture line being variable from one specimen to

918   another. Parasphenoid, sphenethmoid, and palatine are fused in most specimens

919   (sphenethmoid seems to extend well beyond the palatine, as also observed in decalcified

920   specimens). The palatine region is singular, bones are fused or closely in contact forming a

921   robust structure; neopalatine is concave and in contact with the parasphenoid medially, the

922   sphenethmoid dorsally, and the vomer anteriorly. Neopalatine fused with vomer in most

923   specimens. Vomer consists of a thin vertical bony lamella parallel to the anterior-posterior

924   axis of the skull.

925   The columella is medially enlarged. The squamosal is T-shaped with a slightly

926   inflated base because of its fusion with the quadratojugal. The zygomatic ramus is slightly

927   less developed and a little bit longer than the otic ramus in most specimens (roughly equal in

928   length in *S. salseri* AMNH89813, more developed in *S. mesomorphus* sp. nov. SMNS12077

929   and *S. mirandaribeiroi* MNHN-RA-1974.0397). Incomplete pterygoid-prootic arch, but both

930   pterygoid and prootic are practically in contact. Incomplete maxillary arch sensu Trueb

931   (2011) which contradicts Nelson and Lescure (1975) and Walker (1973) but is in accordance

932   with Carvalho (1954) and Zweifel (1986) who reported the quadratojugal and the maxilla not

933   being in contact. Squamosal with a laterally inflated base which could be the quadratojugal,

934   both forming a concavity where the angulospenial inserts. Well-developed pterygoid

935   overlapping to half of the length of the maxilla(Fig. 10; Fig. S2). The anterior part of the

936   pterygoid is imbricated into the maxilla. The posterior part of the pterygoid is firmly in

937   contact with the medial ramus of the squamosal. Pterygoid body deep, slightly arched in

938   dorsal view, bearing a mediodorsal tuberosity and a deep lateral groove; posterior and medial

939   rami poorly differentiated. Maxillary well-developed, thicker near the nasal region, and

940   protruding well beyond the mandible. The ventral part of the premaxilla is curved. The allary

941   process of the premaxilla is long and inclined forward (angle between the base and the tip of

942   the process ≈ 140°). Septomaxilla present, rounded ventrally and notched posteriorly.

943   The mandible is acuminate, slightly arched ventrally, posteriorly thicker, the dentary is

944   slim and overlaps half the length of the angulosplenial, which extends slightly beyond the

945   squamosal and the quadratojugal. Small mentomeckelians with the characteristic microhylid

946   well-developed meckelian diverticulum, slightly longer than mentomeckelians, and parallel to

947   the mandible.

948

949   *3.2.3. Interspecific variation in cranial characteristics.* Except from size differences among

950   species (relative size: *Synapturanus zombie* sp. nov. (n = 2) > *S. ajuricaba* sp. nov. (n = 2) >

951   *S. mirandaribeiroi* (n = 3) > *S. mesomorphus* sp. nov. (n = 4) > *S. salseri* (n = 1)), skull shape

952   is overall conserved among species, with a few variable characteristics, nonetheless. The

953   cranium of *Synapturanus* sp. "Ecuador" is substantially more elongated (HW < HL), less

954   ossified, and more acuminate in dorsal view than in other *Synapturanus* species (cranium

955   truncate or rounded in shape and cranial bones more heavily fused in the other species).

956   *Synapturanus* sp. "Juami" has a rounded skull shape (vs. truncate in the species of the eastern

957   clade), a shorter snout (the nasal bones do not extend laterally as in other species).

958   *Synapturanus salseri* and *S. mesomorphus* sp. nov. differ from *S. mirandaribeiroi*, *S. zombie*

959   sp. nov. and *S. ajuricaba* sp. nov. by having less conspicuous depressions on the prootic and

960   frontoparietal. Sphenoid-nasal bridge and septum is more ossified in *S. mirandaribeiroi*, *S.*

961   *zombie* sp. nov. and *S. ajuricaba* sp. nov. than in the other species (Fig. 10; Fig. S2).

962   *Synapturanus* sp. "Ecuador" differs from other species by having a shorter medial ramus of

963   the squamosal, a thickening of the top medial ramus region of the squamosal and a more

964   developed otic ramus than the zygomatic ramus. *Synapturanus* sp "Juami" differs from other

965   species by having a well-developed and shorter otic ramus with an arched and longer

966   zygomatic ramus and by having the anterior part of the maxilla thicker than its posterior part.

967   Furthermore the anterior part of the maxilla in S. sp. "Juami" doesn't extend beyond the

968   premaxilla like in the other species (Fig. 11; Fig S3).

969

970   *3.2.4. Vertebrae.* Nine vertebrae (eight presacral + one sacral); presacral vertebrae

971   procoelous; eighth vertebra (V8) amphicoelous (Fig. 11; Fig. S3). Atlas and axis well sculpted

972   and developed, axis with short transverse processes, distally enlarged. V3 transversal

973   processes with a dorsal medial apophysis. The neural spine is bulbous in V1–2, with a ridge in

974   V3–5 and smooth in V6–8. Sacral diapophyses rounded. Smooth ilia and urostyle. Urostyle

975   ridge present, extending on ¾ of its length.

976

977   *3.2.5. Interspecific variation in vertebral characteristics. Synapturanus* sp. "Ecuador" differs

978   from the other species by having a relatively small atlas (16 < HL/AL <17) being only

979   slightly sculpted (cf. below). *Synapturanus* sp. "Juami" and *S. salseri* differ from *S.*

980   *mesomorphus* sp. nov., *S. mirandaribeiroi*, *S. ajuricaba* sp. nov. and *S. zombie* sp. nov. by

981   having a relatively medium-sized (12 < HL/AL < 13) and moderately sculpted atlas (Fig. 11;

982   Fig. S3). *Synapturanus mesomorphus* sp. nov. differs from *S. mirandaribeiroi*, *S. ajuricaba*

41

983   sp. nov. and *S. zombie* sp. nov. by having a moderately sculpted atlas despite sharing with

984   them a relatively large atlas (8 < HL/AL < 10). In *Synapturanus mirandaribeiroi, S. ajuricaba*

985   sp. nov. and *S. zombie* sp. nov., the atlas is larger and more developed with a bulbous neural

986   spine and a depression on each side of the vertebral body, and the posterior neural arch bears

987   a crest starting from the post zygapophysis, extending to the neural spine. Additionally,

988   *Synapturanus salseri, S*. sp. "Juami" and *S*. sp. "Ecuador" differ from *S. mirandaribeiroi, S.*

989   *zombie, S. ajuricaba* and *S. mesomorphus* by having an atlas with a longer axis process with

990   no enlarged terminal part and shorter lateral processes of trunk vertebrae V–VIII. In *S. salseri*

991   and *S*. sp. "Juami" the lateral processes are only slightly shorter while in *S*. sp "Ecuador" they

992   are distinctly much shorter, being half of the length of the ones of *S. salseri* and *S*. sp "Juami"

993   and less than half of the length of ones of other species.

994   Two specimens (SMNS12077 and SMNS12078) of *Synapturanus mesomorphus* have

995   the sacrum with straight edges (vs. rounded in other species and in other *S. mesomorphus*

996   specimens). MCP13775 (*S*. sp. "Juami") has a malformation on the left part of the sacrum

997   (Fig. 11; Fig. S3).

998

999   *3.2.6. Pectoral girdle.* Base and anterior part of the suprascapula partially ossified. Clavicle

1000   absent (Fig. 12; Fig. S4). Scapula and coracoid completely fused without evidence of suture

1001   except in two specimens: *S. ajuricaba* INPA-H38464 and *S. mirandaribeiroi* MNHN-RA-

1002   1974.0397. Short humerus associated with an enlarged deltopectoral crest. Short and thick

1003   radio-ulna. Ulna and radius well-developed, ulna thicker than radius (Fig. 12; Fig. S4).

1004   Prepollex present, composed of two bones, the proximal one is rounded, whereas the distal

1005   one is acuminate anteriorly (Fig. 13; Fig. S4). Element Y large, as big as the ulnare.

1006   Metacarpals and phalanges I and II distally enlarged. Terminal phalanges pointed.

1007

1008   *3.2.7. Interspecific variation in pectoral girdle. Synapturanus* sp. "Ecuador" differs from the

1009   other species by having a lower ratio of humerus/radio-ulna length (ratio humerus/radio-ulna

1010   for *S.* sp. "Ecuador" H/R < 1.80 vs. constant among other species examined H/R ≈ 2). Radio-

1011   ulna is thus proportionally longer in *Synapturanus* sp. "Ecuador". Relative size of enlarged

1012   dectopectoral crest and capitulum as follows: *S. ajuricaba* sp. nov. > *S. zombie* sp. nov .> *S.*

1013   *mirandaribeiroi* > *S. mesomorphus* sp. nov. > *S. salseri* > *S.* sp. "Juami" > *S.* sp. "Ecuador"

1014   suggesting different modalities in fossoriality (Fig. 12; Fig. S4). Prepollex laterally protruding

1015   in *S. zombie* sp. nov.*, S. ajuricaba* sp. nov., *S. mirandaribeiroi, S. mesomorphus* sp. nov. and

1016   *S. salseri* (vs. poorly developed in *S.* sp. "Ecuador and *S.* sp. "Juami"). Combined length of

1017   phalanges I and II of Finger III longer than metacarpals in *S. ajuricaba* sp. nov., *S. zombie* sp.

1018   nov. and *S. mirandaribeioi* (metacarpal length 115–125% of phalanges I + II vs. 94–112% in

1019   *S. mesomorphus* sp. nov., *S. salseri*, *S.* sp. "Juami" and *S.* sp. "Ecuador") (Fig. 13; Fig. S5).

1020   All these differences suggest more pronounced fossoriality.

1021

1022   *3.2.8. Pelvic girdle.* Tibio-fibula is the longest bone in the pelvic girdle, slightly longer than

1023   the femur (mean across all specimens F/TF = 0.92 (SD =0.03)), femur and tibio-fibula smooth

1024   (Fig. 14; Fig. S6). Condyles of the femur and tibio-fibula slightly larger distally than

1025   proximally. Tarsal region well ossified. Prehallux present. Absence of crista femoralis in all

1026   species. Tarsal epiphysis well developed, distal tarsal bones relatively reduced in size

1027   compared to the prehallux/element Y; d3 is slender and d1–d2 are small, oval. Prehallux

1028   composed of two juxtaposed bones, the distal one is slender, the proximal one is rectangular

1029   lying on the element Y, which is well developed and thicker than d3.

1030

1031   *3.2.9. Interspecific variation in pelvic girdle. Synpaturanus* sp. "Ecuador" has a distinctly

1032   fused tibiale and fibulare (vs. fused only in distal and proximal apophyses in the other

43

1033 species) (Fig. 14; Fig. S6). This fusion is also present in the other species (*S. rabus* - R.

1034 Keeffe pers. com., *S*. sp. "Divisor", *S*. sp. "Ecuador") of the western clade and probably

1035 represent a synapomorphy for that clade. Despite this unique fusion, the pelvic girdle

1036 elements are generally similar among all examined *Synapturanus*.

1037

1038 **4. Discussion**

1039

1040 *4.1. Species diversity in Synapturanus*

1041 The discovery of phenotypically differentiated unnamed species in Amazonia is far from

1042 surprising. Most studies that have explored the question of how many species exist in

1043 particular groups of amphibians, (e.g., Gehara et al., 2014; Fouquet et al., 2016; Kok et al.,

1044 2017; Vacher et al., 2017; Jaramillo et al., 2020), including Microhylidae (e.g., Peloso et al.,

1045 2014; de Sá et al., 2020), have uncovered high numbers of unnamed species. In many cases,

1046 the initial recognition of diversity is based on genetic data (commonly based on a single or

1047 very few genes), but after closer examination most of the genetic lineages also present

1048 conspicuous phenotypic diagnostic characters (Peloso et al., 2014; Fouquet et al., 2014; Kok

1049 et al., 2016; Carvalho et al., 2021). Therefore, it is likely that many new taxa will continue to

1050 be discovered through the integrative use of DNA sequences and detailed phenotypic

1051 analyses, progressively unveiling the unknown diversity of Amazonian amphibians.

1052 A recent DNA-based species delimitation work suggested that three to four times

1053 more species of frogs than formally recognized occur in Amazonia (Vacher et al., 2020).

1054 Moreover, a recent study targeted at uncovering the diversity within *Synapturanus* found 18

1055 lineages that could correspond to distinct species (Fouquet et al., 2021). These 18 lineages

1056 included 12 that were also phenotypically distinct (based on morphology and/or

1057 advertisement call data), and therefore recognized as *Confirmed Candidate Species* (CCS;

1058 Vieites et al., 2009). However, only three names were available for these candidate species

1059 within *Synapturanus*. The higher proportion of unnamed species in *Synapturanus* (six times)

1060 than in Amazonian frogs in general (four times) likely stems from the combination of the

1061 challenge in finding these secretive frogs (resulting is scarcity of specimens in collections and

1062 of natural history data), from the high regional endemism in the genus, and from the fact that

1063 the group has been taxonomically neglected for quite some time.

1064   Herein, we named three of the species suggested as CCS by Fouquet et al. (2021), for

1065 a total of six formally recognized taxa in *Synapturanus*. There is, however, evidence

1066 suggesting that additional *Synapturanus* species may have not been included by Fouquet et al.

1067 (2021), most notably the large-bodied species from Colombia identified as *S. mirandaribeiroi*

1068 by Pyburn (1975). We also obtained call recordings from Rio Juruá and Novo Airão

1069 (Amazonas, Brazil) that display unique characteristics and deserve additional scrutiny.

1070 Finally, the conspecificity of the populations from French Guiana and Suriname identified as

1071 *S. mirandaribeiroi* with the ones from northern Amazonas in Brazil remains ambiguous

1072 considering acoustic differences.

1073   Therefore, it seems that the more we gather material and information, the more

1074 candidate species are unveiled in *Synapturanus*. Extensive work remains to be undertaken to

1075 describe the extant diversity in this genus, which implies to sample additional populations and

1076 not only specimens but molecular, acoustic and natural history data. We hope that this new

1077 contribution will encourage and facilitate further species descriptions in this extremely

1078 interesting and intriguing genus.

1079

1080 *4.2. Morphological evolution and fossoriality in Synapturanus*

1081 Fouquet et al. (2021) identified three distinct osteological phenotypes within *Synapturanus*,

1082 based on the morphology of the skull and humerus. One of these phenotypes (phenotype 3) is

1083 found in the easternmost species of the eastern clade, i.e., the clade that includes *S.*

1084 *mirandaribeiroi*, *S. zombie*, *S. hades*, and two other candidate species south of the Amazon

1085 River. *Synapturanus salseri*, *S. mesomorphus* and another candidate species (*S.* sp. "Neblina")

1086 are distributed more westward and display a somewhat intermediate phenotype (phenotype 2),

1087 even though these species are included in the eastern clade. The examination of external and

1088 osteological variation across species as presented herein, led us to further characterize

1089 morphological evolutionary trends that are likely linked to behavioral differences across

1090 species, notably differences in fossoriality.

1091   Reinforcement of the skull and the humerus in the species with phenotype 3 was

1092 previously identified in Fouquet et al. (2021). This trend is also evident in various additional

1093 structures examined herein, notably the atlas, the scapula-coracoid and the radio-ulna. The

1094 atlas and the posterior part of the head are strongly sculpted and the scapula-coracoid and

1095 radio-ulna are distinctly thicker in *S. hades*, *S. zombie* and *S. mirandaribeiroi*. These features

1096 could be linked with the insertion of larger muscles. The fusion of the scapula and the

1097 coracoid have been reported in several lineages of frogs. Notably, in the fossorial *Hemisus*

1098 (Engelkes et al., 2020) and in the semifossorial *Hamptophryne* (de Sá and Trueb, 1991) and

1099 may provide a strong, fixed arch against which the muscles of the shoulder and arm brace to

1100 enable digging. These characteristics are seemingly accompanied by a reduction of the size of

1101 phalanges, more developed fringes on the fingers, smaller eyes and an increase in body size,

1102 altogether suggesting an overall increase of the fossorial habits of these species (Emerson,

1103 1976; Mendoza et al., 2019; Thomas et al., 2020). In contrast, the differences in the posterior

1104 part of the body are subtle among all *Synapturanus* species. In the absence of behavioral

1105 observations, and thus on the sole basis of morphology, it remains speculative to discuss the

1106 nuances in the digging behavior across species. Nevertheless, it seems very likely that all

1107 *Synapturanus* dig head-first. We also speculate that the easternmost species (associated with

46

phenotype 3) have reinforced anterior bones and modified soft tissue on hand and snout

compared to the other species either because they dig deeper, longer galleries, or simply

because they spend more time underground or because the soil where they occur is

mechanically more challenging to dig in. These hypotheses are not mutually exclusive, and

need to be corroborated or rejected by actual field or laboratory observations.

Although meager, existing field observations suggest behavioral differences among

the species having these distinct phenotypes. Western species, including *S. mesomorphus* and

S. salseri, seem to be more epigean and have been more frequently observed exposed on the

ground surface, either foraging or migrating for breeding. They were also collected with high

success using pitfall trapping. In comparison, we have never seen a single specimen of *S.

mirandaribeiroi*, *S. ajuricaba* or *S. zombie* above the ground surface. More fossorial habits in

these easternmost species are corroborated by very short calling activity vs. apparently more

prolonged and opportunistic calling activity observed in *S. salseri*, *S. mesomorphus* and

Synapturanus spp. of the western clade. As far as we know, calling is circumscribed to a few

hours during rain showers preceding the rainy season (November–December) in *S. zombie*.

An additional observation is that we often found female specimens while digging in

search of calling males in this group of species. We thus hypothesized female vocalization

and/or the possibility of reproductive fidelity over long periods and biparental care, a rare

mating system in frogs (de Sá et al., 2020). Since we can reasonably speculate that finding a

mate requires migrating at the surface in *Synapturanus*, the cost of such movements for

reproduction may be reduced by reproductive fidelity. We additionally note that sexual

dimorphism is very subtle in these easternmost species. In comparison, body size and

proportion differences in the species of the western and central clades are conspicuous. This

may also be the consequence of both sexes being fossorial in the easternmost species with

both male and female digging galleries and foraging underground whereas this behavior may

1133 be different among sexes in western species. The limited data available on the diet of *S.*

1134 *ajuricaba* (herein), *S. salseri* (Pyburn, 1975), *S. rabus* (Pyburn, 1977), *S. mirandaribeiroi*, *S.*

1135 *mesomorphus* (Nelson and Lescure, 1975) suggest myrmecophagy in the entire genus that

1136 could take place either underground or above the ground surface, thus not providing more

1137 insight on the matter of degree of fossoriality.

1138 The species forming the western clade (including *S. rabus*) share phenotype 1,

1139 characterized by a slender cranium and humerus (Fouquet et al., 2021). These species are also

1140 the smallest, and Pyburn (1977) noticed that they also display comparatively larger eyes than

1141 other species. They have been hypothesized to be the most epigean. In this paper we only

1142 thoroughly examined one of the candidate species included in that clade (*S.* sp. "Ecuador") for

1143 comparison with the newly described species. However, it is noteworthy that all species of the

1144 western clade examined in Fouquet et al. (2021) share a fusion of the tibiale and fibulare

1145 throughout their entire lengths to form a fused bone structure. This condition is only found in

1146 several Centrolenidae genera (Guayasamin et al., 2009) and in Pelodytidae (Sanchiz et al.,

1147 2002) (see also Duellman and Trueb, 1994), two families that are not fossorial and display

1148 high jumping performances. This fusion may thus confer the *Synapturanus* of the western

1149 clade strong jumping abilities related to their leaf-litter habitat (Fabrezi et al., 2017). Mendoza

1150 et al. (2019) found that jumping power declines more rapidly with body mass in burrowing

1151 species of frogs than non-burrowing species and suggested the existence of a functional trade-

1152 off between jumping and burrowing performance. Therefore, the smaller size of these species

1153 compared to the ones of the eastern clade also strengthens the idea that they are more epigean.

1154

References

Audacity Team (2020). Audacity(R): Free Audio Editor and Recorder [Computer application]. Version 2.4.2 retrieved Sep 20th 2020 from https://audacityteam.org/

Ávila-Pires, T.C.S.D., Hoogmoed, M.S., Rocha, W.A.D. 2010. Notes on the vertebrates of northern Pará, Brazil: a forgotten part of the Guianan Region, I. Herpetofauna. Boletim do Museu Paraense Emílio Goeldi, 5, 13–11.

Barrio-Amorós, C.L., Brewer-Carías, C. 1999. Geographic distribution: *Synapturanus mirandaribeiroi*. Herpetological review 30, 51.

Barrio-Amorós, C.L., Brewer-Carías, C., Fuentes-Ramos, O. 2011. Aproximación preliminar a la herpetocenosis de un bosque pluvial en la sección occidental de la Sierra de Lema, Guyana Venezolana. Revista de Ecología Latinoamericana 16, 1–46.

1206 Barrio-Amorós, C.L., Rojas-Runjaic, F. J.M., Señaris, J.C. 2019. Catalogue of the amphibians

1207   of Venezuela: Illustrated and annotated species list, distribution, and conservation.

1208   Amphibian and Reptile Conservation 13, 1–198.

1209 Boulenger, G.A. 1882. Catalogue of the Batrachia Salientia s. Ecaudata in the Collection of

1210   the British Museum. Second Edition. London: Taylor and Francis.

1211 Boulenger, G.A. 1900. Batrachians. In E. R. Lankester, Report on a collection made by

1212   Messrs. F. V. McConnell and J. J. Quelch at Mount Roraima in British Guiana.

1213   Transactions of the Linnean Society of London. 2nd series, Zoology 8, 55–56.

1214 Carvalho, A.L. de. 1954. A preliminary synopsis of the genera of American microhylid frogs.

1215   Occasional Papers of the Museum of Zoology, University of Michigan 555, 1–19.

1216 Carvalho, T.R., Moraes, L.J., Lima, A.P., Fouquet, A., Peloso, P.L., Pavan, D., Drummond,

1217   L.O., Rodrigues, M.T., Giaretta, A.A., Gordo, M., Neckel-Oliveira, S. 2021.

1218   Systematics and historical biogeography of Neotropical foam-nesting frogs of the

1219   *Adenomera heyeri* clade (Leptodactylidae), with the description of six new Amazonian

1220   species. Zoological Journal of the Linnean Society, 191, 395–433.

1221 Cole, C. J., Townsend, C.R., Reynolds, R.P., MacCulloch, R.D., Lathrop, A. 2013.

1222   Amphibians and reptiles of Guyana, South America: illustrated keys, annotated

1223   species accounts, and a biogeographic synopsis. Proceedings of the Biological Society

1224   of Washington 125, 317–578.

1225 Dewynter, M., Courtois, A.E., Villette, B. 2019. La base de données Faune-Guyane.

1226   Amphibiens et Reptiles. 2018 : première synthèse. 294p.

1227 Dezécache, C., Faure, E., Gond, V., Salles, J. M., Vieilledent, G., Hérault, B. 2017. Gold-rush

1228   in a forested El Dorado: deforestation leakages and the need for regional cooperation.

1229   Environmental Research Letters 12, 034013.

1230 Emerson, S.B. 1976. Burrowing in frogs. Journal of Morphology 149, 437–458.

Engelkes, K., Kath, L., Kleinteich, T., Hammel, J. U., Beerlink, A., & Haas, A. 2020. Ecomorphology of the pectoral girdle in anurans (Amphibia, Anura): Shape diversity and biomechanical considerations. Ecology and evolution 10, 11467–11487.

Ernst, R., Rödel, M., Arjoon, D. 2005. On the cutting edge-the anuran fauna of the Mabura Hill Forest Reserve, central Guyana. Salamandra 41, 179.

Ernst, R., Linsenmair, K.E., Rödel, M.O. 2006. Diversity erosion beyond the species level: dramatic loss of functional diversity after selective logging in two tropical amphibian communities. Biological Conservation 133(2), 143–155.

Fitzinger, L.J.F.J. 1843. Systema Reptilium. Fasciculus Primus. Wien: Braumüller et Seidel.

Fabrezi, M., Alberch, P. 1996. The carpal elements of anurans. Herpetologica 52, 188–204.

Fabrezi, M., Goldberg, J., Chuliver Pereyra, M. 2017. Morphological variation in anuran limbs: constraints and novelties. Journal of Experimental Zoology Part B: Molecular and Developmental Evolution 328, 546–574.

Fouquet, A., Martinez, Q., Courtois, E.A., Dewynter, M., Pineau, K., Gaucher, P., Blanc, M., Marty, C., Kok, P.J.R. 2013. A new species of the genus *Pristimantis* (Amphibia, Craugastoridae) associated with the moderately elevated massifs of French Guiana. Zootaxa 3750, 569–586.

Fouquet, A., Martinez, Q., Zeidler, L., Courtois, E.A., Gaucher, P., Blanc, M., Lima, J.D., Souza, S.M., Rodrigues, M.T., Kok, P.J.R. 2016. Cryptic diversity in the *Hypsiboas semilineatus* species group (Amphibia, Anura) with the description of a new species from the eastern Guiana Shield. Zootaxa 4084, 79–104.

Fouquet, A., Leblanc, K., Framit, M., Réjaud, A., Rodrigues, M.T., Castroviejo-Fisher, S., Peloso, P.LV., Prates, I., Manzi, S., Suescun, U., Baroni, S., Moraes, L.J.C.L., Recoder, R., de Souza, S.M., Dal Vecchio, F., Camacho, A., Guellere, J.M., Rojas-Runjaic, F.J.M., Gagliardi-Urrutia, G., de Carvalho, V.T., Gordo, M., Menin, M., Kok,

1256   P.J.R, Hrbek, T., Werneck, F.P., Crawford, A.J., Ron, S.R., Mueses-Cisneros, J.J.,

1257   Rojas Zamora, R.R., Pavan, D., Simões, P.I., Ernst, R., Fabre, A.C. 2020. Species

1258   diversity and biogeography of an ancient frog clade from the Guiana Shield (Anura:

1259   Microhylidae: *Adelastes*, *Otophryne*, *Synapturanus*) exhibiting spectacular phenotypic

1260   diversification. B.J.L.S., laa204, https://doi.org/10.1093/biolinnean/blaa204

1261 Frost, D.R. 2021. Amphibian Species of the World: an Online Reference. Version 6.1 (01

1262   January   2021).   Electronic   Database   accessible   at

1263   https://amphibiansoftheworld.amnh.org/index.php. American Museum of Natural

1264   History, New York, USA. doi.org/10.5531/db.vz.0001

1265 Gehara, M., Crawford, A.J., Orrico, V.G., Rodríguez, A., Lötters, S., Fouquet, A., Barreintos,

1266   L.S., Brusquetti, F., De la Riva, I., Ernst, R., Gagliardi-Urrutia, G., Glaw, F.,

1267   Guayasamin, J.M., Hölting, M., Jansen, M., Kok, P.J.R., Kwet, A., Lingnau, R., Lyra,

1268   M., Moravec, J., Pombal, J.P. Jr., Rojas-Runjaic, F.J.M., Schulze, A., Señaris, J.C.,

1269   Solé, M., Rodrigues, M.T., Twomey, E., Haddad, C.F.B., Vences, M., Köhler, J. 2014.

1270   High levels of diversity uncovered in a widespread nominal taxon: continental

1271   phylogeography of the Neotropical tree frog *Dendropsophus minutus*. PloS one 9,

1272   p.e103958.

1273 Gosner, K.L. 1960. A simplified table for staging anuran embryos and larvae with notes on

1274   identification. Herpetologica 16, 183–190.

1275 Guayasamin, J.M., Castroviejo-Fisher, S., Trueb, L., Ayarzagüena, J., Rada, M., Vila, C.,

1276   2009. Phylogenetic systematics of Glassfrogs (Amphibia: Centrolenidae) and their

1277   sister taxon *Allophryne ruthveni*. Zootaxa 2100, 1–97.

1278 IUCN. 2020. The IUCN Red List of Threatened Species. Version 2020-3.

1279   https://www.iucnredlist.org. Downloaded on 10 March 2020.

1280   Jaramillo, A.F., De La Riva, I., Guayasamin, J.M., Chaparro, J.C., Gagliardi-Urrutia, G.,

1281   Gutiérrez, R.C., Brcko, I., Vilà, C., Castroviejo-Fisher, S. 2020. Vastly underestimated

1282   species richness of Amazonian salamanders (Plethodontidae: *Bolitoglossa*) and

1283   implications about plethodontid diversification. Molecular Phylogenetics and

1284   Evolution 149, p.106841.

1285   Keeffe, R., Blackburn, D.C. 2020. Comparative morphology of the humerus in forward-

1286   burrowing frogs. Biological Journal of the Linnean Society 131, 291–303.

1287   Köhler, J., Jansen, M., Rodríguez, A., Kok, P.J.R., Toledo, L.F., Emmrich, M., Glaw, F.,

1288   Haddad, C.F.B., Rödel, M.-O., Vences, M. 2017. The use of bioacoustics in anuran

1289   taxonomy: theory, terminology, methods and recommendations for best practice.

1290   Zootaxa 4251, 1–124.

1291   Kok, P.J.R., Kalamandeen, M. 2008. Introduction to the taxonomy of the amphibians of

1292   Kaieteur National Park, Guyana. Abc Taxa 5, 1–278.

1293   Kok, P.J.R., Russo, V.G., Ratz, S., Means, D.B., MacCulloch, R.D., Lathrop, A., Aubret, F.,

1294   Bossuyt, F. 2017. Evolution in the South American "Lost World": insights from

1295   multilocus phylogeography of stefanias (Anura, Hemiphractidae, *Stefania*). Journal of

1296   Biogeography 44, 170–181.

1297   Kok, P.J.R., Russo, V.G., Ratz, S., Aubret, F. 2016. On the distribution and conservation of

1298   two "Lost World" tepui summit endemic frogs, *Stefania ginesi* Rivero, 1968 and *S.*

1299   *satelles* Señaris, Ayarzagüena, and Gorzula, 1997. Amphibian and Reptile

1300   Conservation 10, 5–12.

1301   Kok, P.J.R., van der Velden, M., Means, D.B., Ratz, S., Josipovic, I., Boone, M., McDiarmid,

1302   R. 2020. Coping with the extremes: comparative osteology of the tepui-associated toad

1303   *Oreophrynella* and its bearing on the evolution of osteological novelties in the genus.

1304   Zoological Journal of the Linnean Society 190, 114139.

1305   Lima, A.P., Magnusson, W.E., Menin, M., Erdtmann, L.K., Rodrigues, D.J., Keller, C., Hödl,

1306   W. 2006. Guia de sapos da Reserva Adolpho Ducke, Amazônia Central. Editora

1307   INPA, Manaus.

1308   Mendoza, E., Azizi, E., Moen, D.S. 2020. What explains vast differences in jumping power

1309   within a clade? Diversity, ecology and evolution of anuran jumping power. Functional

1310   Ecology 34, 1053–1063.

1311   Menin, M., Rodrigues, D.J., Lima, A.P. 2007. Clutches, tadpoles and advertisement calls of

1312   *Synapturanus mirandaribeiroi* and *S*. cf. *salseri* in Central Amazonia, Brazil.

1313   Herpetological Journal 17, 86–91.

1314   Menin, M, Waldez, F, Lima, A.P. 2008. Temporal variation in the abundance and number of

1315   species of frogs in 10,000 ha of a forest in central Amazonia, Brazil. South American

1316   Journal of Herpetology 3, 68–81.

1317   Neckel-Oliveira, S., Gordo, M. 2004. Anfíbios, lagartos e serpentes do Parque Nacional do

1318   Jaú. In: Borges HS, Iwanaga S, Durigan CC, Pinheiro MR (eds.). Janelas para a

1319   Biodiversidade no Parque Nacional do Jaú: uma estratégia para o estudo da

1320   biodiversidade na Amazônia. Manaus: Fundação Vitória Amazônica, pp. 161–176.

1321   Nelson, C.E. 1973. Systematics of the Middle American upland populations of *Hypopachus*

1322   (Anura: Microhylidae). Herpetologica 29, 6–17.

1323   Nelson, C.E., Lescure, J. 1975. The taxonomy and distribution of *Myersiella* and

1324   *Synapturanus* (Anura: Microhylidae). Herpetologica 31, 389–397.

1325   Ouboter, P.E., Jairam, R. 2012. Amphibians of Suriname. Brill, Leiden, 376 pp.

1326   Peloso. P.L.V., Sturaro, M.J, Forlani, M., Motta, A.P., Gaucher, P., Wheeler, W.C. 2014.

1327   Phylogeny, taxonomic revision, and character evolution of the genera *Chiasmocleis*

1328   and *Syncope* (Anura, Microhylidae) in Amazonia, with descriptions of three new

1329   species. Bulletin of the American Museum of Natural History 386, 1–96.

1330   Peloso, P.L.V., Frost, D.R., Richards, S.J., Rodrigues, M.T., Donnellan, S., Matsui, M.,

1331   Raxworthy, C.J., Biju, S.D., Lemmon, E.M., Lemmon, A.R., Wheeler, W.C. 2016.

1332   The impact of anchored phylogenomics and taxon sampling on phylogenetic inference

1333   in narrow-mouthed frogs (Anura, Microhylidae). Cladistics 32, 113–140.

1334   Pyburn, W.F. 1975. A new species of microhylid frog of the genus *Synapturanus* from

1335   southeastern Colombia. Herpetologica 31, 439–443.

1336   Pyburn, W.F. 1977 "1976". A new fossorial frog from the Colombian rainforest (Anura:

1337   Microhylidae). Herpetologica 32, 367–370.

1338   Rojas-Zamora, R.R., Fouquet, A., Ron, S.R., Hernández-Ruz, E.J., Melo-Sampaio, P.R.,

1339   Chaparro, J.C., Vogt, R.C., de Carvalho, V.T., Pinheiro, L.C., Ávila, R.W., Farias,

1340   I.P., Gordo, M., Hrbek, T. 2018. A Pan-Amazonian species delimitation: high species

1341   diversity within the genus Amazophrynella (Anura: Bufonidae). PeerJ 6(e4941), 1–56.

1342   de Sá, F.P., Consolmagno, R.C., Muralidhar, P., Brasileiro, C.A., Zamudio, K.R., Haddad,

1343   C.F. 2020. Unexpected reproductive fidelity in a polygynous frog. Science advances

1344   6(33), p.eaay1539.

1345   de Sá, R.O., Trueb, L. 1991. Osteology, skeletal development, and chondrocranial structure of

1346   *Hamptophryne boliviana* (Anura: Microhylidae). Journal of Morphology 209, 311–

1347   330.

1348   Sanchiz, B., Tejedo, M., Sánchez-Herráiz, M.J. 2002. Osteological differentiation among

1349   Iberian *Pelodytes* (Anura, Pelodytidae). Graellsia 58, 35–68

1350   Souza, M. 2019. História da Amazônia. Do período pré-Colombiano aos desafios do Século

1351   XXI. 391p. Ed. Record, Rio de Janeiro.

1352   Thomas, K.N., Gower, D.J., Bell, R.C., Fujita, M.K., Schott, R.K., Streicher, J.W. 2020. Eye

1353   size and investment in frogs and toads correlate with adult habitat, activity pattern and

1354   breeding ecology. Proceedings of the Royal Society B 287(1935), p.20201393.

1355 Trueb, L. 1968. Cranial osteology of the hylid frog, *Smilisca baudini*. University of Kansas

1356   Publications, Museum of Natural History 18, 11–35.

1357 Trueb, L. 1973. Bones, frogs, and evolution. In: Vial, J.L. (Ed.), Evolutionary biology of the

1358   anurans: Contemporary research on major problems. University of Missouri Press,

1359   USA, pp. 65–132.

1360 IUCN 2020. The IUCN Red List of Threatened Species. Version 2020-1.

1361   https://www.iucnredlist.org. Downloaded on [01 01 2020].

1362 Vacher, J.-P., Chave, J., Ficetola, F.G., Sommeria-Klein, G., Tao, S., Thébaud, C., Blanc, M.,

1363   Camacho, A., Cassimiro, J., Colston, T.J., Dewynter, M., Ernst, R., Gaucher, P.,

1364   Gomes, J.O., Jairam, R., Kok, P.J.R., Lima, J.D., Martinez, Q., Marty, C., Noonan,

1365   B.P., Nunes, P.M.S., Ouboter, P., Recoder, R., Rodrigues, M.T., Snyder, A., Marques-

1366   Souza, S., Fouquet, A. 2020. Large scale DNA-based survey of frogs in Amazonia

1367   suggests a vast underestimation of species richness and endemism. Journal of

1368   Biogeography 47, 1781–1791.

1369 Vacher, J.-P., Kok, P.J.R., Rodrigues, M.T., Dias Lima, J., Lorenzini, A., Martinez, Q., Fallet,

1370   M., Courtois, E.A., Blanc, M., Gaucher, P., Dewynter, M., Jairam, R., Ouboter, P.,

1371   Thébaud, C., Fouquet, A. 2017. Cryptic diversity in Amazonian frogs: integrative

1372   taxonomy of the genus *Anomaloglossus* (Amphibia: Anura: Aromobatidae) reveals a

1373   unique case of diversification within the Guiana Shield. Molecular Phylogenetics and

1374   Evolution 112, 158–173.

1375 Vieites, D.R., Wollenberg, K.C., Andreone, F., Köhler, J., Glaw, F., Vences, M. 2009. Vast

1376   underestimation of Madagascar's biodiversity evidenced by an integrative amphibian

1377   inventory. Proceedings of the National Academy of Sciences 106, 8267–8272.

1378 Walker, C.F. 1973. A new genus and species of microhylid frog from Ecuador. Occasional

1379   Papers of the Museum of Natural History, University of Kansas 20, 1–7.

1380   Wassersug, R., Pyburn, W.F. 1987. The biology of the Pe-ret toad, *Otophryne robusta*

1381   (Microhylidae), with special consideration of its fossorial larva and systematic

1382   relationships. Zoological Journal of the Linnean Society 91, 137–169.

1383   Zweifel, R.G. 1986. A new genus and species of microhylid frog from the Cerro de la Neblina

1384   region of Venezuela and a discussion of relationships among New World microhylid

1385   genera. American Museum novitates 2863, 1–24.

1386

1388
1389 **Table 1.** Morphological measurements in mm (individual measurements are available in
1390 Appendix D).

			SVL	HL	HW	IO	IN	EN	ED	FAL	HAND	ThL	TL	FL
S. mirandaribeiroi	M (n=14)	Mean	29.1	5.7	6.1	3.7	1.9	2.0	1.5	4.4	4.9	10.7	10.8	10.9
		min	26.6	5.2	4.9	3.3	1.7	1.7	1.3	3.7	4.2	8.2	9.8	9.6
		max	30.8	6.5	6.5	4.0	2.1	2.2	1.7	4.9	5.6	12.4	12.2	11.9
	F (n=3)	Mean	31.5	6.1	6.5	3.8	2.0	2.1	1.5	4.5	5.2	11.4	11.4	11.3
		min	28.6	5.9	5.8	3.4	1.9	2.0	1.3	3.6	4.5	10.5	10.3	10.3
		max	34.4	6.4	7.6	4.1	2.1	2.2	1.6	5.0	5.9	12.6	12.6	12.9
S. zombie sp. nov.	M (n=5)	Mean	39.2	7.4	7.5	4.8	2.4	2.4	1.5	5.7	7.1	14.4	13.8	13.9
		min	37.0	7.3	7.2	4.4	2.2	2.0	1.4	5.1	6.8	13.7	13.1	13.5
		max	40.6	7.7	7.8	5.1	2.6	2.7	1.6	6.5	7.4	15.2	15.1	14.4
	F (n=2)	Mean	40.5	7.0	7.7	4.7	2.5	2.5	1.6	5.7	7.0	13.5	13.6	13.5
		min	39.0	6.9	7.7	4.6	2.4	2.4	1.6	5.6	6.7	12.5	13.4	13.4
		max	42.1	7.1	7.7	4.9	2.5	2.6	1.7	5.9	7.2	14.4	13.8	13.5
S. mesomorphus sp. nov.	M (n=4)	Mean	24.8	5.0	5.2	3.0	1.8	1.7	1.4	3.6	4.0	8.8	10.0	10.8
		min	23.0	4.8	5.1	2.9	1.7	1.6	1.3	3.3	3.8	8.3	9.1	9.4
		max	26.0	5.1	5.5	3.1	1.8	1.9	1.6	3.8	4.2	9.5	10.7	13.1
	F (n=7)	Mean	28.0	5.5	5.6	3.3	1.8	1.8	1.5	4.0	4.7	9.7	11.3	10.9
		min	27.1	4.7	5.1	3.0	1.5	1.6	1.2	3.5	4.3	8.5	10.8	10.0
		max	29.4	6.3	6.5	3.7	1.9	2.1	1.6	4.5	4.9	10.7	11.8	11.6
S. ajuricaba sp. nov.	M (n=5)	Mean	31.8	6.1	6.2	3.7	1.9	2.5	1.6	4.9	5.4	11.8	11.8	11.3
		min	29.3	5.9	5.8	3.5	1.8	2.3	1.6	4.7	5.2	11.1	10.8	10.6
		max	33.2	6.4	6.6	3.9	2.1	2.6	1.7	5.3	5.7	12.5	12.7	12.0
	F (n=3)	Mean	36.5	6.3	7.0	4.3	2.5	2.5	1.7	5.7	5.8	12.1	12.2	11.7
		min	35.9	6.2	6.7	4.2	2.3	2.3	1.6	5.4	5.7	11.4	11.7	10.9
		max	37.3	6.5	7.3	4.3	2.6	2.6	1.7	6.0	5.9	12.6	12.7	12.4

1391
1392
1393 **Table 2.** Acoustic variables.

		NL (s)	DoF (Hz)	Pulses	DeF (Hz)	internote
S. rabus (n=1)	NA	0.039	1642	1	169	11.20
S. salseri (n=6)	Mean	0.079	1411	1	49	5.31
	min	0.071	1312	1	14	2.36
	max	0.090	1574	1	91	9.16
S. mirandaribeiroi (n=9)	Mean	0.167	1251	7	148	6.57
	min	0.130	1100	5	22	4.10
	max	0.194	1471	8	256	11.56
S. zombie sp. nov. (n=4)	Mean	0.154	1107	1	142	8.48
	min	0.147	1059	1	104	6.90
	max	0.167	1190	1	194	9.90
S. mesomorphus sp. nov.(n=2)	Mean	0.167	1093	1	28	10.30
	min	0.160	1058	1	15	9.66
	max	0.173	1127	1	40	10.93
S. ajuricaba sp. nov. (n=5)	Mean	0.322	1064	14	57	6.91
	min	0.282	1013	12	11	5.20
	max	0.366	1121	16	87	9.04
S. sp. "Timbo" (n=1)	NA	0.107	1017	1	21	5.22

1394

Appendix A: Museum acronyms

MZUSP: Museum of Zoology of the University of São Paulo, Brazil; AMNH: American Museum of Natural History, USA; MNHN-RA: The reptiles and amphibians collection (RA) of the Muséum national d'Histoire Naturelle, France; UMMZ: University of Michigan Museum of Zoology, USA; INPA: Instituto Nacional de Pesquisas da Amazônia, Brazil; UTA: Herpetological Collections at the University of Texas at Arlington, USA; USNM: Smithsonian Institution, National Museum of Natural History, USA; ANDES: Universidad de los Andes, Colombia; MTD: Museum of Zoology Senckenberg Dresden, Germany; SMNS: State Museum of Natural History Stuttgart, Germany; RBINS: Royal Belgian Institute of Natural Sciences, Belgium; MPEG: Museu Paraense Emílio Goeldi, Brazil; CM: Carnegie Museum, USA; UT: University of Texas at Austin, USA; QCAZ: Museo de Zoología de la Pontificia Universidad Católica del Ecuador; Ecuador; MCP: Museu de Ciências e Tecnologia da Pontifícia Universidade Católica do Rio Grande do Sul, Brazil.

Appendix B: Additional material examined

Synapturanus mirandaribeiroi

Non type specimens (16 specimens)

MNHN-RA-2020.0079 (AF2791) MNHN-RA-2020.0080 (AF2844) MNHN-RA-2020.0082 (AF3975) three males from Mitaraka (2.2358°N 54.4493°W); MNHN-RA-2020.0081 (AF2845); MNHN-RA-2020.0083 (AF3732) and MNHN-RA-2020.0084 (AF3758) a female and two males from Voltzberg, Suriname; INPA-H10890, INPA-H11837, INPA-H11843, INPA-H11867, INPA-H13169, INPA-H13170, INPA-H19781, seven males from Reserva Florestal Adolpho Ducke (2.9661°S 59.9312°W); INPA-H34023 a male from Mata Goiabinha Av. das Torres (2.9610°S 60.0037°W); INPA-H18572 a female from Parque

1420 Estadual Rio Negro Setor Sul (2.7255°S 60.4045°W); INPA-H37891 a female from

1421 Assentamento Rio Pardo (1.7092°S 60.4387°W).

1422

1423 *Synapturanus* sp. "Timbo"

1424 UTA-A-3987 (Photos by Gregory Pandelis) and UTA-A-4009 (Photos by Gregory Pandelis),

1425 two males from Timbo, Vaupes, Colombia.

1426

1427 *Synapturanus mesomorphus*

1428 **Non type specimens**

1429 RBINS15790 (PK3513), a male collected by M. Wilkinson, D. Gower and P.J.R. Kok on the

1430 17th of March 2011 in Iwokrama Forest Reserve, Guyana (4.3302°N 58.7984°W);

1431 RBINS15810, RBINS15813 (PK3544, PK3547), two males collected by M. Wilkinson, D.

1432 Gower and P.J.R. Kok on the 21st of March 2011 in Iwokrama Forest Reserve, Guyana

1433 (4.3302°N 58.7984°W); RBINS15789 (PK3512), a female collected by M. Wilkinson, D.

1434 Gower and P.J.R. Kok on the 17th of March 2011 in Iwokrama Forest Reserve, Guyana

1435 (4.3302°N 58.7984°W); RBINS15812 (PK3546), a female collected by M. Wilkinson, D.

1436 Gower and P.J.R. Kok on the 21st of March 2011 in Iwokrama Forest Reserve, Guyana

1437 (4.3302°N 58.7984°W); PK3789 (uncatalogued), a juvenile collected by J. Pinto and P.J.R.

1438 Kok on the 30th of November 2012 in Iwokrama Forest Reserve, Guyana (4.4128°N

1439 58.7840°W); MW11578 a male and MW11576–77, MW11579 three females collected by M.

1440 Wilkinson, D. Gower and P.J.R. Kok on the 1st of March 2011 at Iwokrama (4.6714°N

1441 58.6850°W), Guyana.

1442

1443

1444   Appendix C: µCT-scans reference numbers

Taxon	Specimen voucher (Field N°)	Sex	Source (www.morphosource.org/Detail/Media Detail/Show/media_id)
Synapturanus salseri	AMNH89813 paratype	M	M55253
Synapturanus mirandaribeiroi	MNHN-RA-1974.0397 paratype	M	M82442
Synapturanus mirandaribeiroi	MNHN-RA-2020.0081 (AF2845)	F	M82487
Synapturanus mirandaribeiroi	MNHN-RA-2020.0084 (AF3758)	M	M82490
Synapturanus zombie	MNHN-RA-2020.0089 (AF3723)	M	M82491
Synapturanus zombie	MNHN-RA-2020.0087 (AF3573)	F	M82495
Synapturanus sp. "Ecuador"	QCAZA2103	F	M83013
Synapturanus sp. "Ecuador"	QCAZA4852	M	M83016
Synapturanus mesomorphus	SMNS12077	M	M82497
Synapturanus mesomorphus	MTD48012	F	M82498
Synapturanus sp. Juami	MCP13775	M	M83885
Synapturanus sp. Juami	MCP13777	F	M83823
Synapturanus ajuricaba	INPA-H38464	F	M82659
Synapturanus ajuricaba	INPA-H35751	F	M82658

1445

1446

1448 Appendix D: Morphometric data for each specimen

Specimen voucher (field N°)	Species	SEX	SVL	HL	HW	IO	IN	EN	ED	FAL	HAND	ThL	TL	FL
INPA-H18572	*S. mirandaribeiroi*	F	28.6	5.92	6	3.81	1.9	2.03	1.45	3.64	4.5	10.49	10.27	10.26
INPA-H37891 (HT8357)	*S. mirandaribeiroi*	F	31.56	6.01	5.8	3.35	2.13	2.22	1.3	4.78	5.24	11.1	11.28	10.8
MNHN-RA-2020.0081 (AF2845)	*S. mirandaribeiroi*	F	34.42	6.35	7.63	4.14	1.99	2.04	1.6	4.99	5.93	12.58	12.62	12.9
INPA-H13170	*S. mirandaribeiroi*	M	26.6	5.59	6.28	3.5	1.85	2.03	1.45	3.95	4.85	10.67	10.3	10.9
MNHN-RA-1974-397	*S. mirandaribeiroi*	M	26.67	5.17	4.85	3.31	1.68	1.73	1.62	4.44	4.85	8.21	9.9	9.58
INPA-H34023	*S. mirandaribeiroi*	M	27.16	5.36	5.86	3.5	1.67	1.88	1.53	4.34	4.2	10.14	9.8	10.07
INPA-H13169	*S. mirandaribeiroi*	M	28.33	5.65	6.35	3.89	2.08	2.11	1.5	4.5	4.7	10.19	10.33	10.7
INPA-H11843	*S. mirandaribeiroi*	M	29.38	5.8	6.13	3.62	1.87	1.93	1.6	4.33	4.8	10.35	9.86	10.1
MNHN-RA-2020.0082 (AF3975)	*S. mirandaribeiroi*	M	29.44	5.63	5.89	3.99	1.83	1.94	1.52	4.79	5.22	11.03	12.15	11.45
MNHN-RA-2020.0079 (AF2791)	*S. mirandaribeiroi*	M	29.52	6.47	6.4	3.89	1.99	1.91	1.5	4.89	5.44	12.06	11.9	11.85
INPA-H19781	*S. mirandaribeiroi*	M	29.57	5.8	6.18	3.84	1.91	2.21	1.57	4.13	5	10.39	10.32	11.2
MNHN-RA-2020.0083 (AF3732)	*S. mirandaribeiroi*	M	29.68	5.77	5.93	3.6	1.79	1.86	1.34	4.74	4.18	11.62	11.44	11.31
INPA-H11837	*S. mirandaribeiroi*	M	29.88	5.17	5.7	3.6	1.95	1.9	1.6	3.7	4.67	10.04	10.15	10.8
INPA-H10890	*S. mirandaribeiroi*	M	29.9	5.47	6.29	3.68	1.93	1.96	1.63	3.97	4.9	10.46	10.44	10.58
MNHN-RA-2020.0084 (AF3758)	*S. mirandaribeiroi*	M	29.96	6.27	6.1	3.86	2.04	1.94	1.5	4.76	5.59	11.99	11.56	11.67
INPA-H11867	*S. mirandaribeiroi*	M	30.7	5.93	6.38	3.54	1.96	2.07	1.67	4.4	4.63	10.4	10.77	10.9
MNHN-RA-2020.0080 (AF2844)	*S. mirandaribeiroi*	M	30.78	6.17	6.45	4.02	1.89	1.87	1.57	4.94	5.53	12.4	11.6	11.5
MZUSP 159220 (MTR24135)	*S. zombie*	F	38.95	6.93	7.7	4.55	2.52	2.43	1.65	5.62	7.19	14.4	13.35	13.54
MNHN-RA-2020.0085 (AF0525)	*S. zombie*	F	42.12	7.14	7.73	4.86	2.43	2.56	1.58	5.87	6.74	12.5	13.83	13.44
MNHN-RA-2020.0087 (AF3573)	*S. zombie*	F	38.73	7.69	7.44	4.7	2.16	2.52	1.5	6.51	7.03	15.15	14.31	14.37
MNHN-RA-2020.0091 (AF3986)	*S. zombie*	M	37.01	7.28	7.17	4.43	2.47	2.27	1.51	5.09	7.38	13.92	13.1	13.66
MNHN-RA-2020.0090 (AF3985)	*S. zombie*	M	39.34	7.43	7.39	4.63	2.5	2	1.55	5.56	7.12	13.73	13.16	13.59
MNHN-RA-2020.0088 (AF3722)	*S. zombie*	M	40.24	7.34	7.5	4.9	2.6	2.74	1.44	5.75	6.78	14.2	13.3	13.46
MNHN-RA-2020.0089 (AF3723)	*S. zombie*	M	40.62	7.37	7.82	5.12	2.28	2.26	1.55	5.68	7.37	15.13	15.12	14.26
(MW11579)	*S. mesomorphus*	F	27.08	5.05	5.35	3.12	1.59	1.63	1.19	3.54	4.31	8.5	11.1	9.98
USNM588793 (BPN3762)	*S. mesomorphus*	F	27.35	5.68	5.85	3.67	1.73	2.09	1.6	3.91	4.7	9.74	10.83	11.63
(MW11576)	*S. mesomorphus*	F	27.39	5.33	5.26	3.15	1.85	1.8	1.22	3.55	4.65	8.81	11.2	10.27
USNM566235	*S. mesomorphus*	F	27.54	6.29	5.75	3.63	1.89	2	1.6	4.35	4.85	10.58	11.23	11.03
MTD49061	*S. mesomorphus*	F	28.41	4.71	5.63	3.04	1.53	1.67	1.62	3.88	4.63	10.6	11.23	11.1
(MW11577)	*S. mesomorphus*	F	28.7	5.34	5.11	3.33	1.79	1.67	1.36	3.96	4.92	9.3	11.5	11.27
MTD48012	*S. mesomorphus*	F	29.35	5.93	6.5	3.08	1.91	1.91	1.62	4.54	4.67	10.65	11.78	11.06
PK 1641	*S. mesomorphus*	F	29.27	5.42	5.91	3.23	1.72	1.97	1.15	3.99	3.96	10.37	10.32	10.92
PK 1396	*S. mesomorphus*	F	26.29	5.08	5.25	2.98	1.31	1.85	1.11	3.7	2.77	9.63	10.67	9.39
PK 1137	*S. mesomorphus*	F	26.51	4.75	5.17	3.15	1.4	1.68	1.46	3.82	3.47	9.58	10.2	9.78
PK 1143	*S. mesomorphus*	F	28.55	5.07	5.09	3.02	1.24	1.45	1.25	3.17	3.01	9.1	10.01	8.81
USNM588794 (BPN3813)	*S. mesomorphus*	M	23	5.01	5.06	3.14	1.66	1.9	1.43	3.8	4.15	8.69	9.14	9.44

(MW11578)	*S. mesomorphus*	M	24.95	4.92	5.12	3.11	1.83	1.66	1.32	3.77	4.09	8.28	10.5	10.26
SMNS12078	*S. mesomorphus*	M	25.4	4.81	5.25	2.95	1.71	1.63	1.55	3.76	4.17	9.47	10.73	10.3
SMNS12077	*S. mesomorphus*	M	25.95	5.09	5.47	2.92	1.81	1.76	1.28	3.26	3.76	8.58	9.6	13.11
PK 1397	*S. mesomorphus*	M	26.04	5.27	4.77	3.13	1.35	1.7	1.17	2.78	2.78	9.98	10.05	8.91
PK 1577	*S. mesomorphus*	M	22.88	4.37	4.9	2.89	1.18	1.59	1.13	3.3	2.89	9.32	9.79	9.71
INPA-H38464	*S. ajuricaba*	F	35.91	6.47	7.03	4.23	2.4	2.5	1.61	5.95	5.7	12.6	12.7	12.35
INPA-H28519	*S. ajuricaba*	F	36.27	6.34	7.3	4.3	2.34	2.32	1.71	5.44	5.87	12.35	12.2	10.9
INPA-H35751	*S. ajuricaba*	F	37.3	6.2	6.7	4.26	2.64	2.62	1.71	5.8	5.75	11.43	11.69	11.7
MPEG29453 (CN370/PT-006)	*S. ajuricaba*	M	29.3	6	6	3.6	1.8	2.4	1.6	4.7	5.2	11.1	11.4	10.6
MPEG29457	*S. ajuricaba*	M	31.6	5.9	5.8	3.5	1.8	2.3	1.6	4.9	5.2	11.2	10.8	11.1
MPEG29456	*S. ajuricaba*	M	32.2	6.4	6.5	3.8	2.1	2.5	1.65	4.8	5.5	11.9	12.1	11.4
MPEG29454 (CN373/PT-007)	*S. ajuricaba*	M	32.9	6.2	5.9	3.9	2.1	2.6	1.65	5.3	5.3	12.5	12.7	12
MPEG29458	*S. ajuricaba*	M	33.2	6.2	6.6	3.8	1.9	2.5	1.6	4.7	5.7	12.1	12.1	11.4

1449

1450

1451

1452
1453 **Fig. 1.** Preserved adult male of *Synapturanus mirandaribeiroi* from Voltzberg, Suriname

1454 (MNHN-RA-2020.0084; field number AF3758), in dorsal view (A), in ventral view (B), same

1455 specimen in life (C) and audio spectrogram and oscillogram from a call recorded at the same

1456 locality (D). Photos by AF.

1457

1458 **Fig. 2.** Distribution of *Synapturanus* in the Eastern Guiana Shield. Symbols outlined in black

1459 indicate localities for which molecular data are available, symbols outlined in white indicate

1460 additional records from the literature [*Synapturanus mirandaribeiroi*: Nelson and Lescure

1461 (1975), Ouboter and Jairam (2012); *S. mesomorphus* sp. nov.: Nelson and Lescure (1975),

1462 Barrio-Amorós et al. (2011); *S. zombie* sp. nov.: Nelson and Lescure (1975); Dewynter et al.

1463 (2019)] for which no molecular data are available and no specimen was examined by us. Stars

1464 indicate type-localities.

1465

1466 **Fig. 3.** Preserved paratype USNM 197435 (Photos by P.P.) of *Synapturanus salseri* in dorsal

1467 (A) and ventral (B) views; photo in life of ANDES-A 4382 (AF4186) a male specimen from

1468 Mitu (C) (photo by AF), Vaupés Colombia; and audio spectrogram and oscillogram from the

1469 same locality (D).

1470

1471 **Fig. 4.** Preserved holotype MNHN-RA-2020.0091 of *Synapturanus zombie* sp. nov. in dorsal

1472 (A) and ventral (B) views, photo of holotype in life (C); and audio spectrogram and

1473 oscillogram of a call of an unvouchered individual recorded from the type locality (D). Photo

1474 in life by M.D.

1475

1476 **Fig. 5.** Variation among specimens of *Synapturanus zombie* sp. nov. in life. Photos by A.F.

1477

1478   **Fig. 6.** Preserved holotype MTD48012 of *Synapturanus mesomorphus* sp. nov. in dorsal (A)

1479   and ventral (B) views; photo in life of RBINS15790 (PK3513) (C); sonogram of a call record

1480   from the type locality (D) (photo in life by P.J.R.K.).

1481

1482   **Fig. 7.** Variation among specimens of *Synapturanus mesomorphus* sp. nov. in life (photos by

1483   M.H. - holotype and P.J.R.K. – RBINS4204 & RBINS15789)

1484

1485   **Fig. 8.** Preserved holotype INPA-H 38464 of *S. ajuricaba* sp. nov. in dorsal (A) and ventral

1486   (B) views; photo in life of an unvouchered specimen (photo by W.E. Magnusson and A.P.

1487   Lima) (C); sonogram of a call record from Reserva Florestal Adolpho Ducke (D).

1488

1489   **Fig. 9.** Variation among specimens of *Synapturanus ajuricaba* sp. nov. (photo of the

1490   Trombetas specimens by Tiago Pezzuti, and of the unvouchered male from Reserva Florestal

1491   Adolpho Ducke by W.E. Magnusson and A.P. Lima).

1492

1493   **Fig. 10.** Variation in the skull of *Synapturanus.* All species shown in dorsal (left), ventral

1494   (center) and lateral (right, skull in left side view) views. One mm scale bars are illustrated for

1495   each view.

1496

1497   **Fig. 11.** Variation in the vertebral column of *Synapturanus.* All species shown in dorsal view.

1498   One mm scale bars are illustrated for each view.

1499

1500   **Fig. 12.** Variation in the pectoral girdle elements of *Synapturanus.* From left to right, pectoral

1501   girdles shown in lateral, and frontal views, right humerus in dorsal view, right radio-ulna in

1502   dorsal view. One mm scale bars are illustrated for each view.

1503

1504 **Fig. 13.** Variation in hand morphology of *Synapturanus.* All species shown in ventral view.

1505 One mm scale bars are illustrated for each view. The additional structures appearing in grey

1506 behind the carpals when they are not totally preserved, correspond to the radiale, the

1507 intermedium, and the ulnare.

1508

1509 **Fig. 14.** Variation in the pelvic girdle elements of *Synapturanus.* From left to right, pelvic

1510 girdles shown in lateral, and ventral views, femur in dorsal view, tibio-fibula and foot

1511 morphology in ventral view. One mm scale bars are illustrated for each view.

1512

(A) (B) MNHN-RA-2020.0084 (AF3758) male, Voltzberg - Suriname

10 mm

(C)

(D)

(A)

(B)
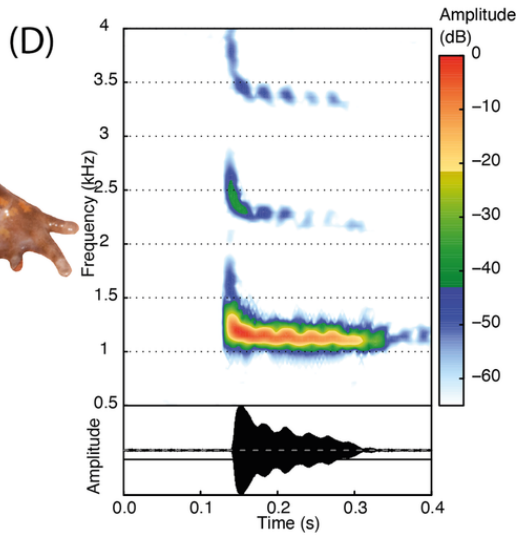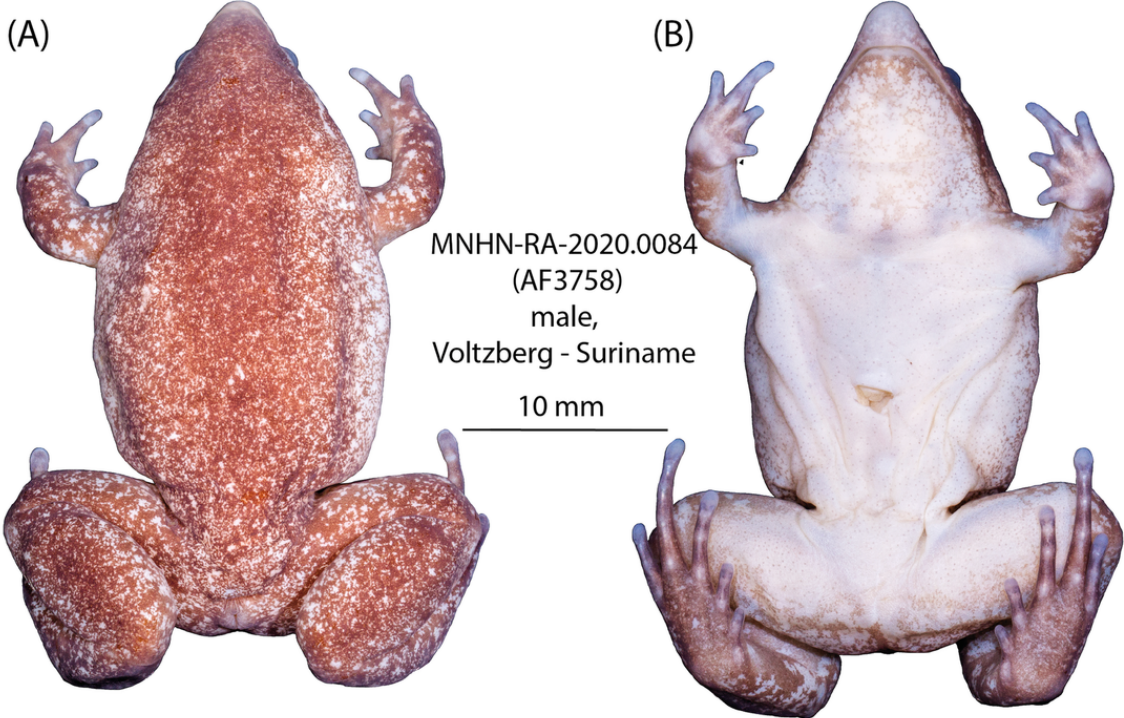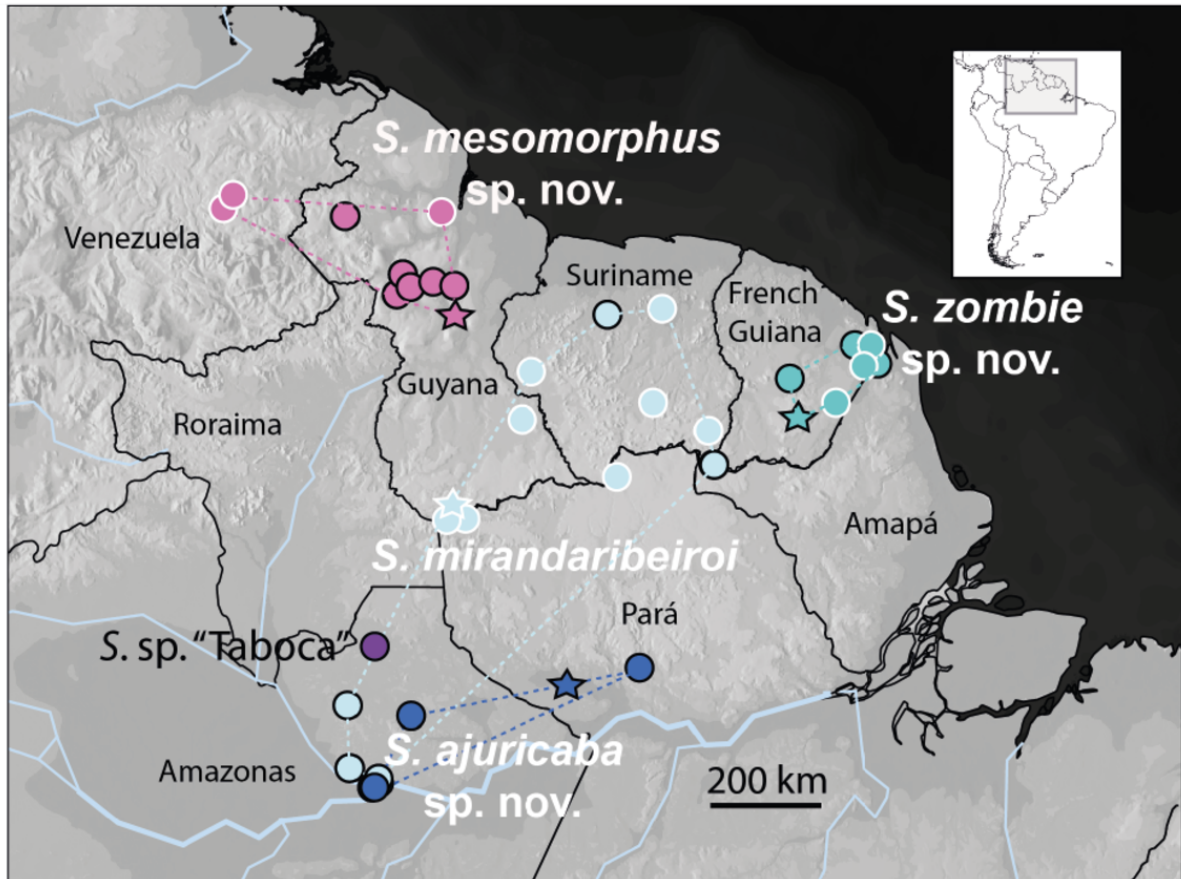
USNM197435
paratype, male,
Timbo, Vaupes - Colombia

10 mm

(C)

ANDES-A4382
male,
Mitu, Vaupes - Colombia

(D)
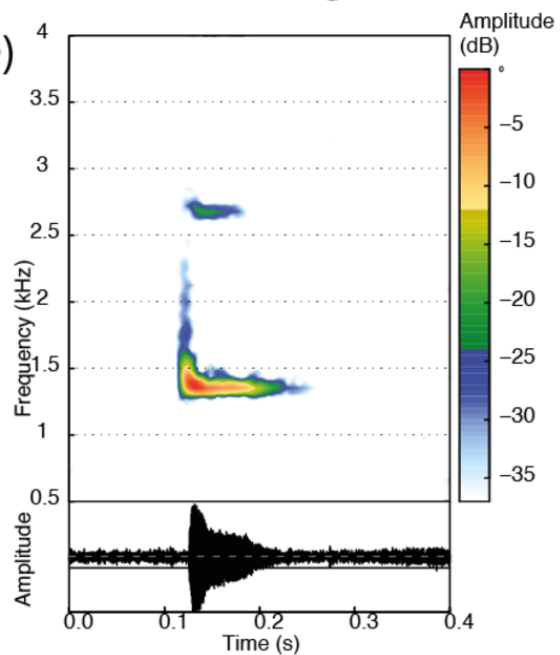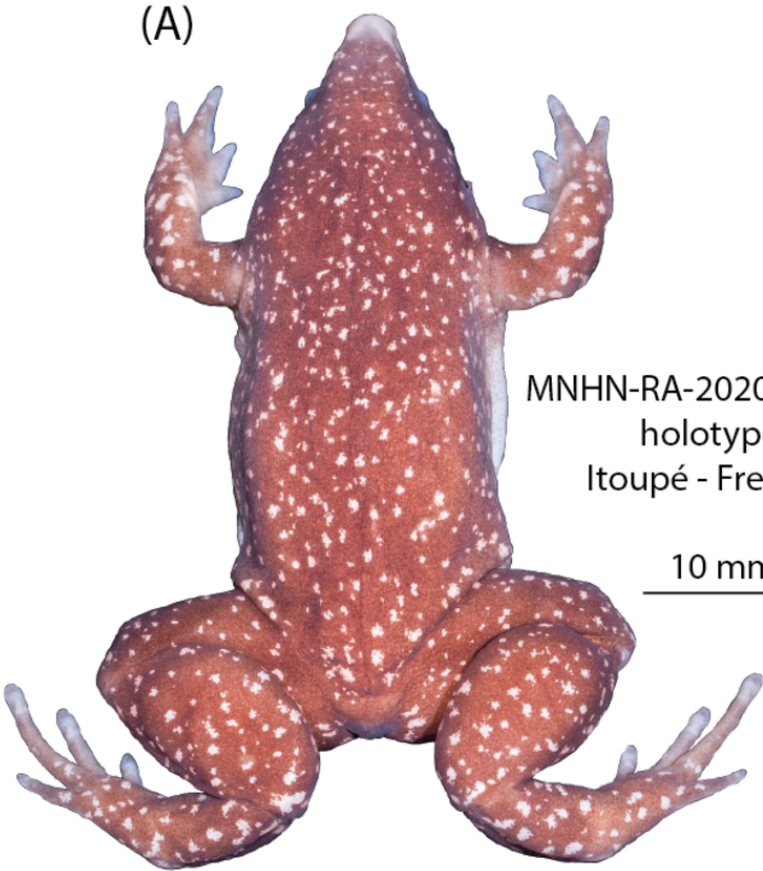
(A), (B) MNHN-RA-2020.0091 (AF3986) holotype, male, Itoupé - French Guiana

10 mm

(C)

(D)
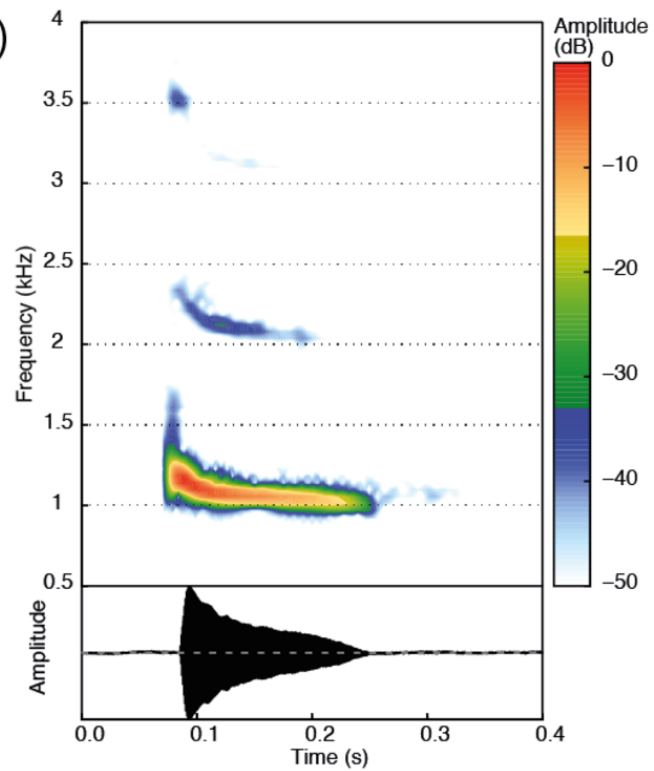
MNHN-RA-2020.0087 (AF3573)
female, Itoupé - French Guiana

MNHN-RA-2020.0087 (AF3723)
male, Itoupé - French Guiana

MZUSP159220 (MTR24135)
female, Oiapoque - Amapa, Brazil

(A) MTD48012 holotype female, Iwokrama - Guyana

10 mm

(C) RBINS15789 male Iwokrama - Guyana

MTD48012 holotype
female,
Iwokrama - Guyana

RBINS4204 paratype
male
Kaieteur NP - Guyana

RBINS15789
female
Iwokrama - Guyana

(A)

(B)
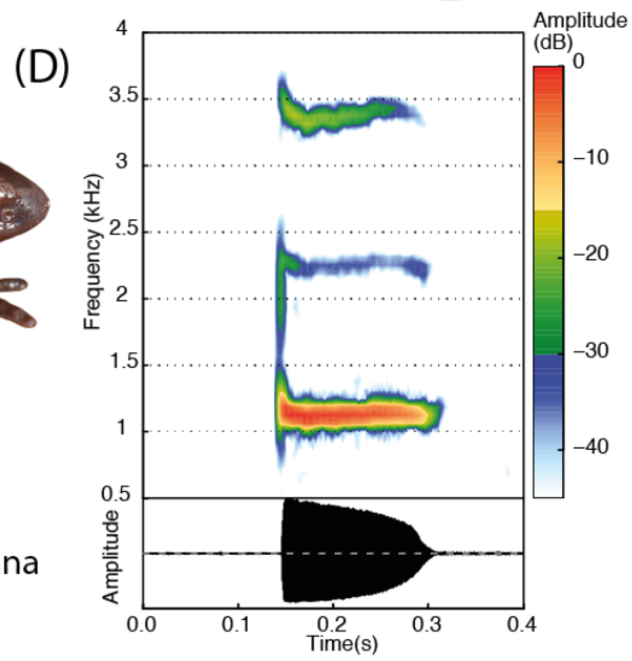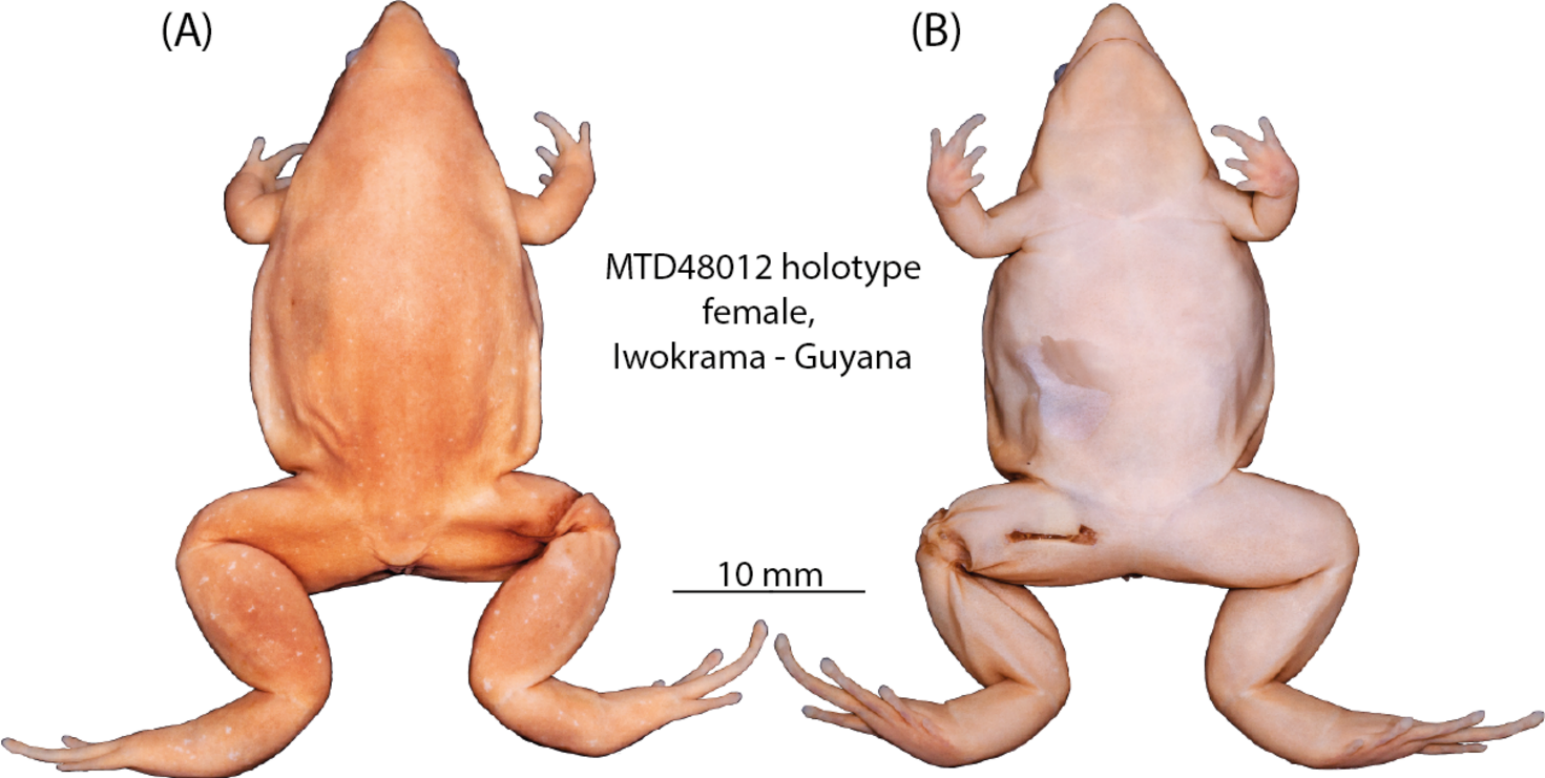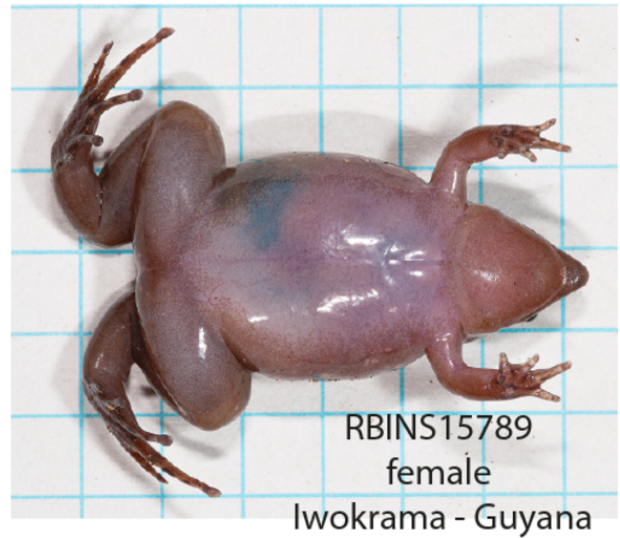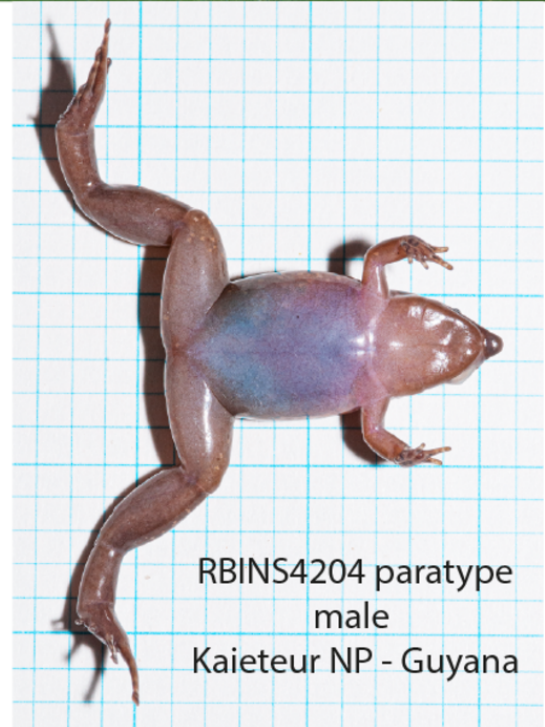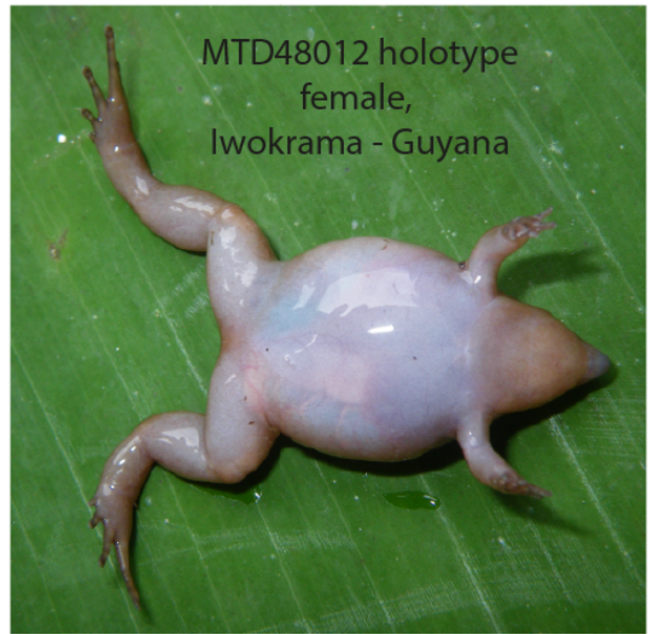
INPA-H38464
holotype, female,
Trombetas, Para - Brazil

10 mm

(C)

Unvouchered male,
Reserva florestal Adolfo Ducke, Amazonas- Brazil

(D)
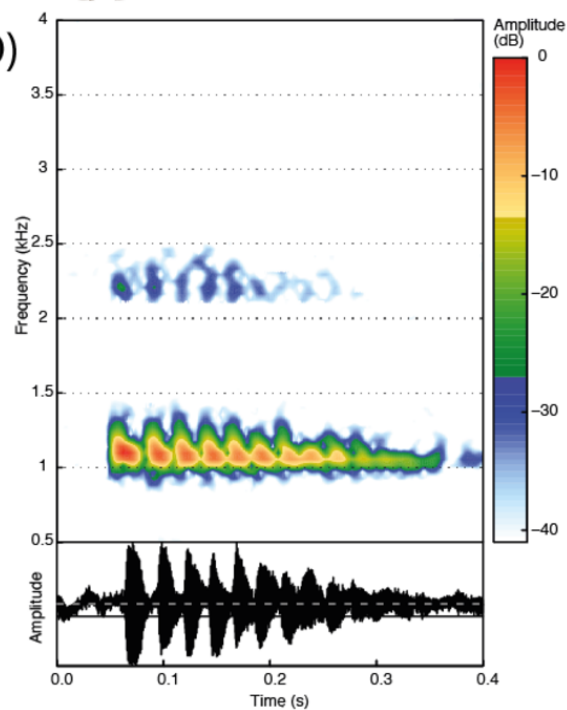
Unvouchered specimen,
Trombetas - Para, Brazil

Unvouchered specimen,
Trombetas - Para, Brazil

Unvouchered male,
RFAD- Amazonas, Brazil

S. mirandaribeiroi male MNHN-RA-2020.0084
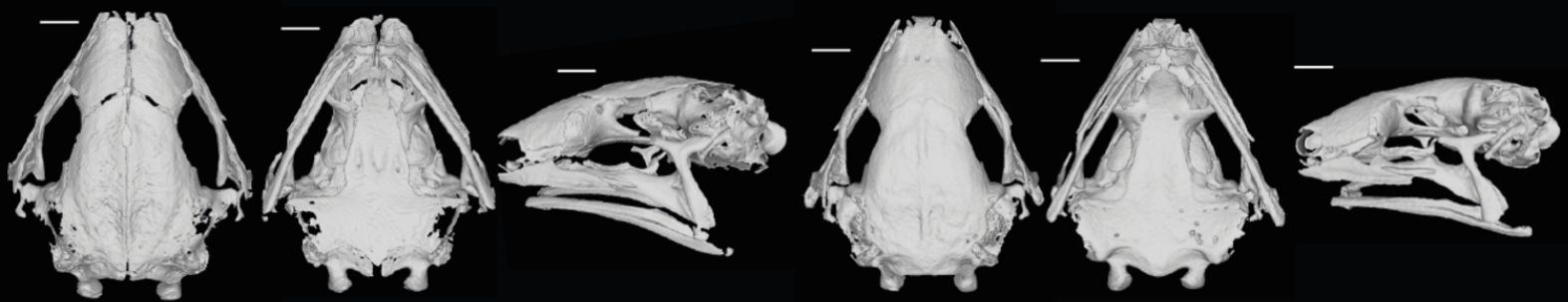
S. mirandaribeiroi male Paratype MNHN-RA-1974.0397

S. salseri male Paratype AMNHN89813

S. zombie sp. nov. male Paratype MNHN-RA-2020.0089

S. ajuricaba sp. nov. female Paratype INPA-H35751

S. mesomorphus sp. nov. male paratype SMNS12077
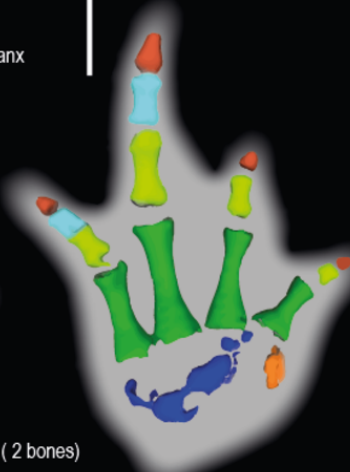
S. sp. " Ecuador" male Q CAZ4852

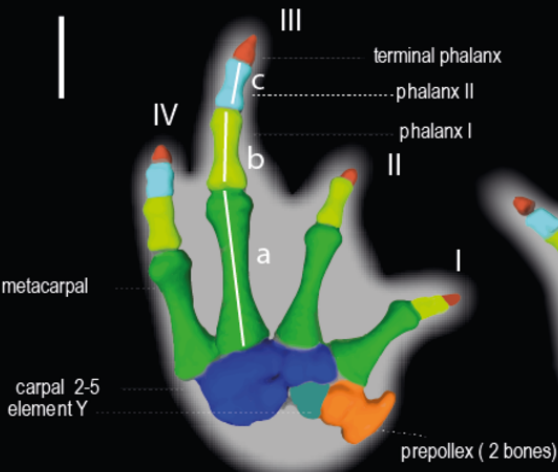*S.* sp. "Juami" male MCP13775

trunk vertebrae

I
II
III
IV
V
VI
VII
VIII

sacral region

S

urostyle

vertebral body depressions

bulbous neural spine

enlarged terminal part

V3 transversal process apophysis

S. mirandaribeiroi male
Paratype MNHN-RA-2020.0084

S. mirandaribeiroi male
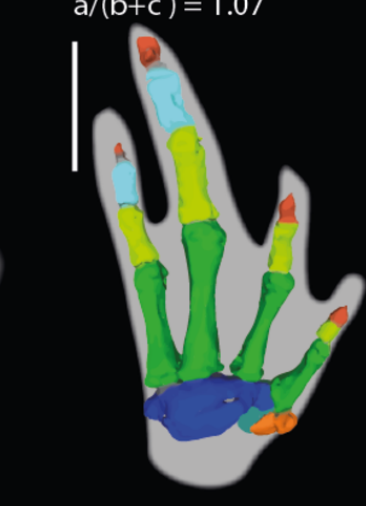Paratype MNHN-RA-1974.0397

S. salseri male
Paratype AMNHN89813
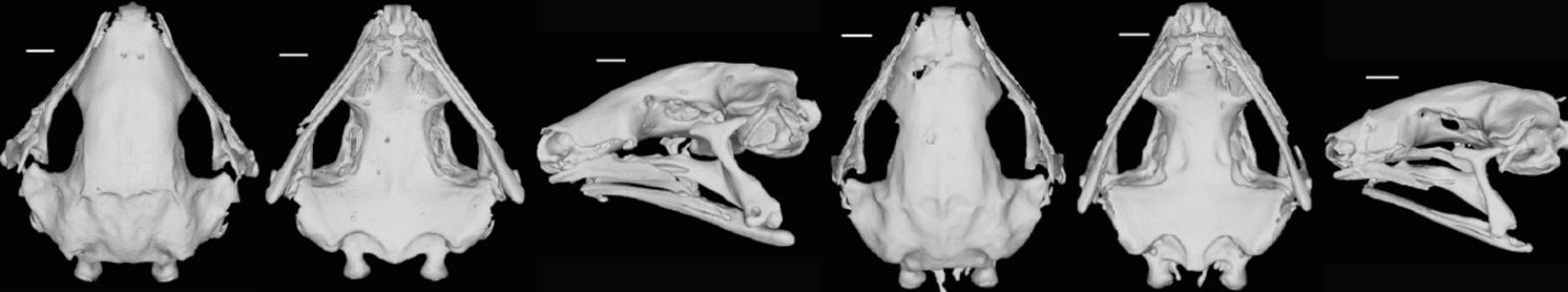
S. zombie sp. nov. male
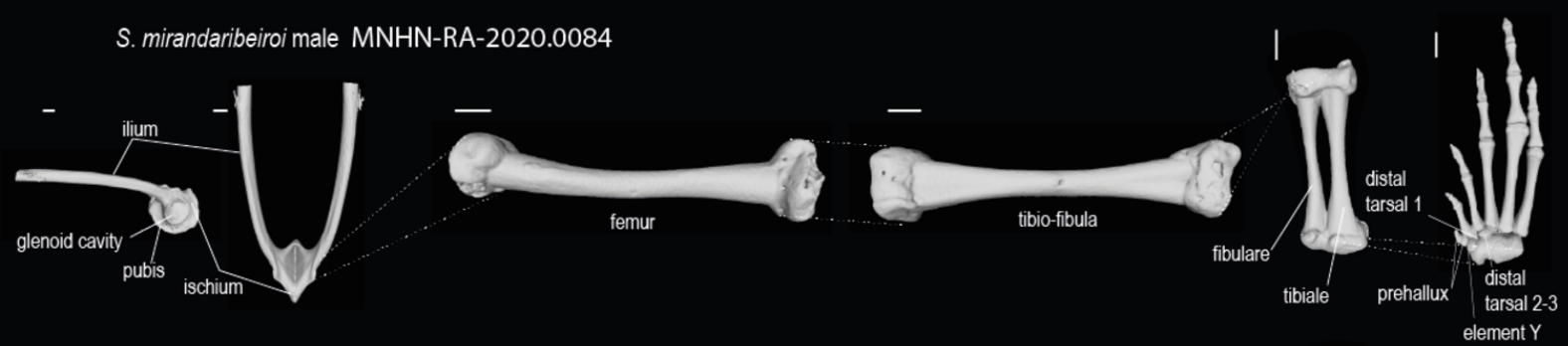Paratype MNHN-RA-2020.0089

S. ajuricaba sp. nov.
female Paratype
INPA-H35751

S. mesomorphus sp. nov. male
Paratype SMNS12077

S. sp. " Ecuador"
male QCAZ4852
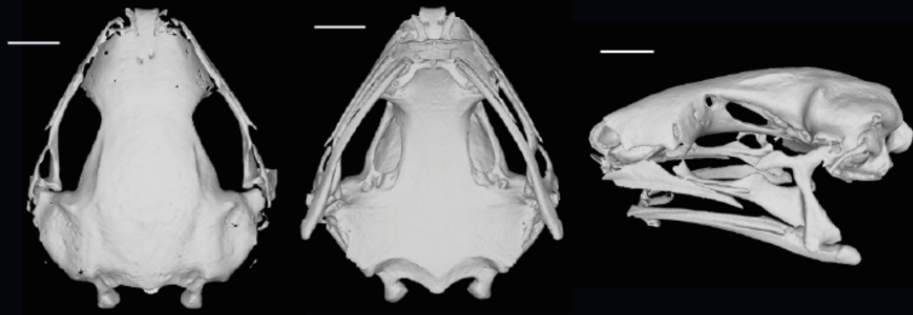
S. sp. "Juami" male
MCP13775

S. *mirandaribeiroi* male MNHN-RA-2020.0084
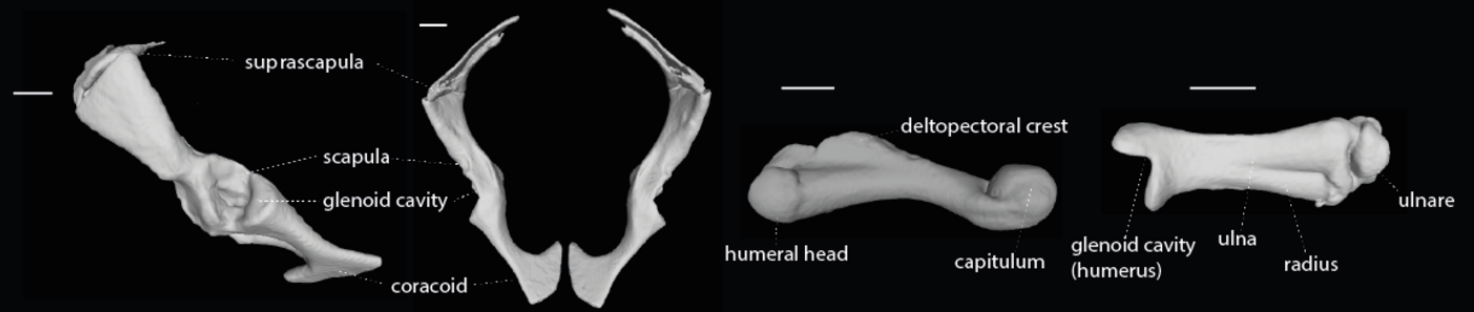
suprascapula
scapula
glenoid cavity
coracoid

deltopectoral crest
humeral head
capitulum
glenoid cavity (humerus)
ulna
radius
ulnare

S. *mirandaribeiroi* male Paratype MNHN-RA-1974.0397
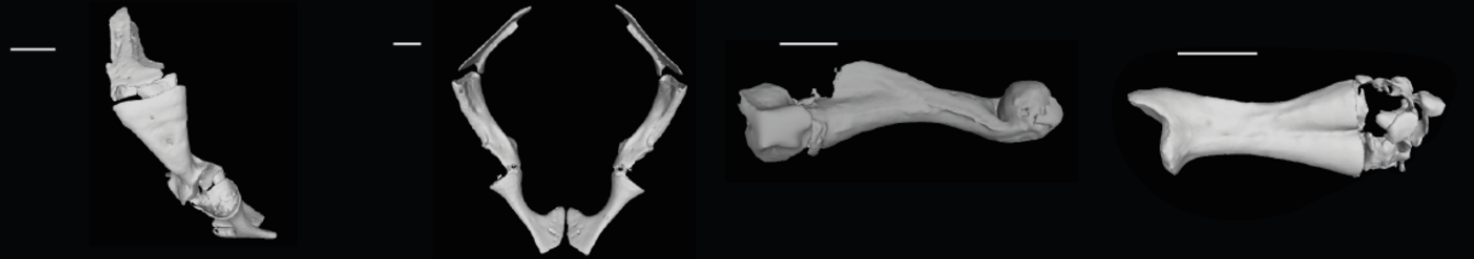
S. *salseri* male Paratype AMNHN89813
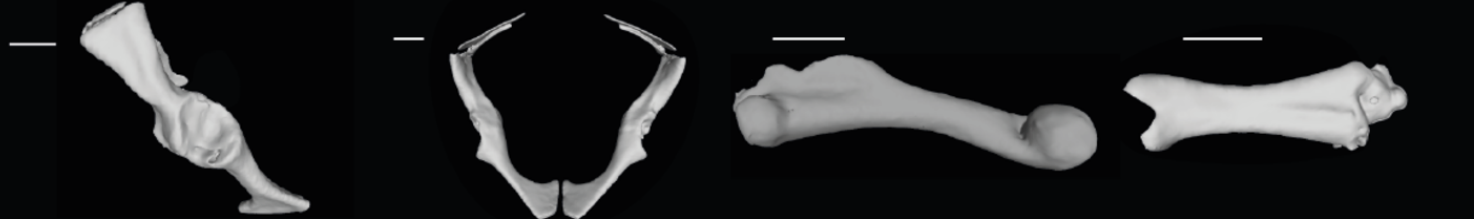
S. *zombie* sp. nov. male Paratype MNHN-RA-2020.0089

S. *ajuricaba* sp. nov. female Paratype INPA-H35751
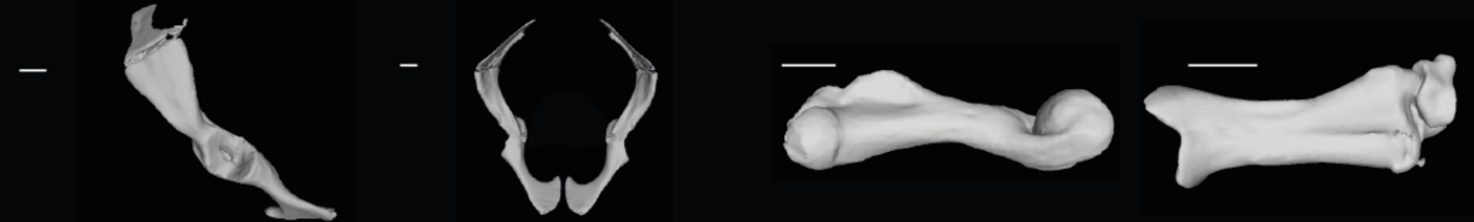
S. *mesomorphus* sp. nov. male paratype SMNS12077
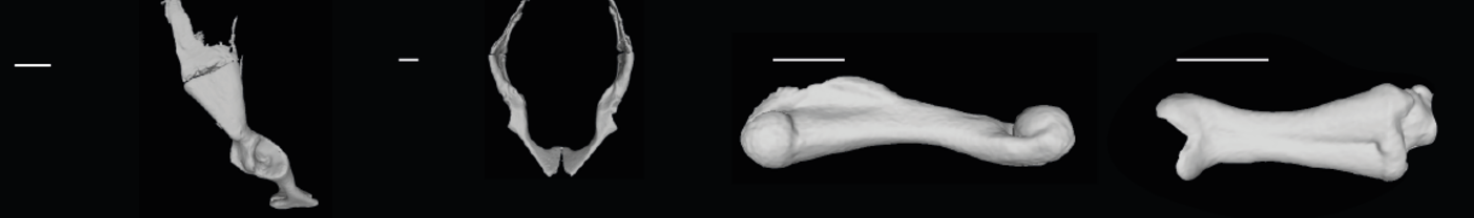
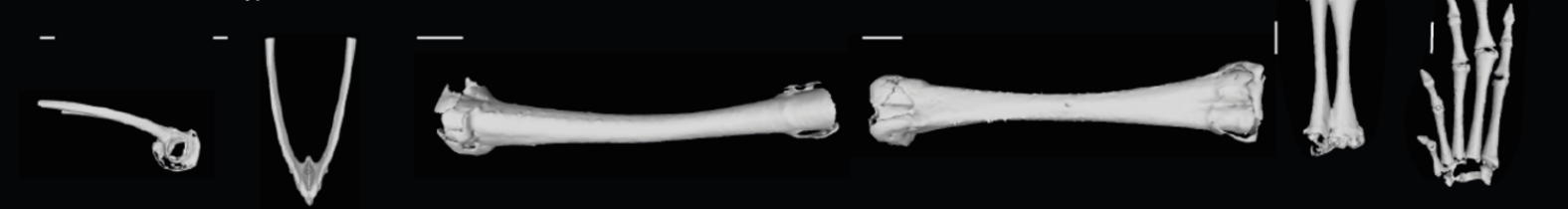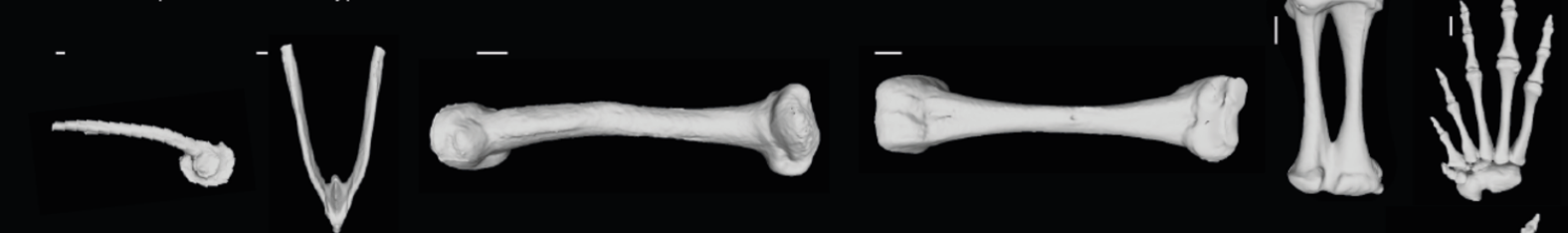S. sp. "Ecuador" male QCAZ4852
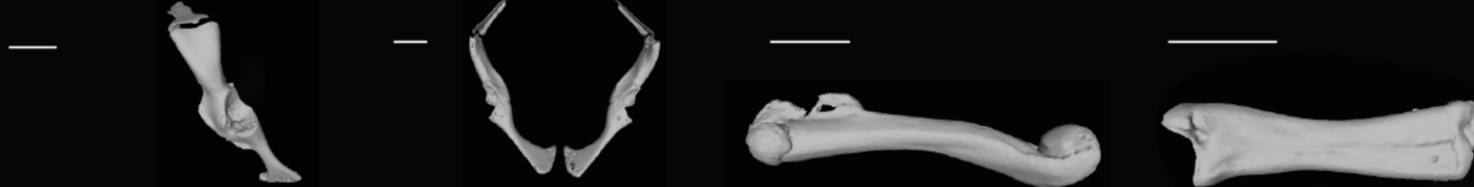
S. sp. "Juami" male MCP13775

a/(b+c) = 1.15

III
terminal phalanx
c
phalanx II
IV
phalanx I
b
II
a
metacarpal
I
carpal 2-5
element Y
prepollex (2 bones)

S. mirandaribeiroi male
MNHN-RA-2020.0084

a/(b+c) = 0.94

S. mirandaribeiroi male
Paratype MNHN-RA-1974.0397

a/(b+c) = 1.21

S. zombie sp. nov.
male Paratype
MNHN-RA-2020.0089

a/(b+c) = 1.16

S. ajuricaba sp. nov.
female Paratype
INPA-H35751

a/(b+c) = 1.06

S. mesomorphus sp. nov.
male paratype
SMNS12077

a/(b+c) = 1.07

S. sp. " Ecuador"
male QCAZ4852

a/(b+c) = 1.12

S. sp. "Juami" male
MCP13775

S. salseri male
Paratype AMNHN89813

S. mirandaribeiroi male MNHN-RA-2020.0084

ilium
glenoid cavity
pubis
ischium
femur
tibio-fibula
distal tarsal 1
fibulare
tibiale
prehallux
distal tarsal 2-3
element Y

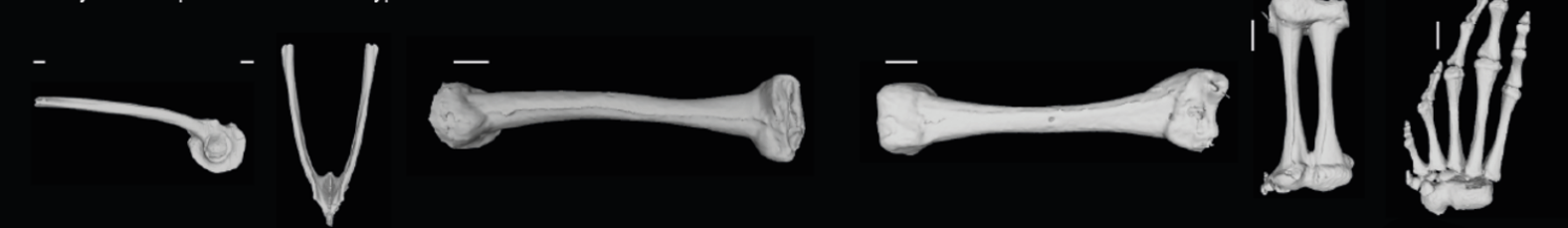*S. mirandaribeiroi* male Paratype MNHN-RA-1974.0397
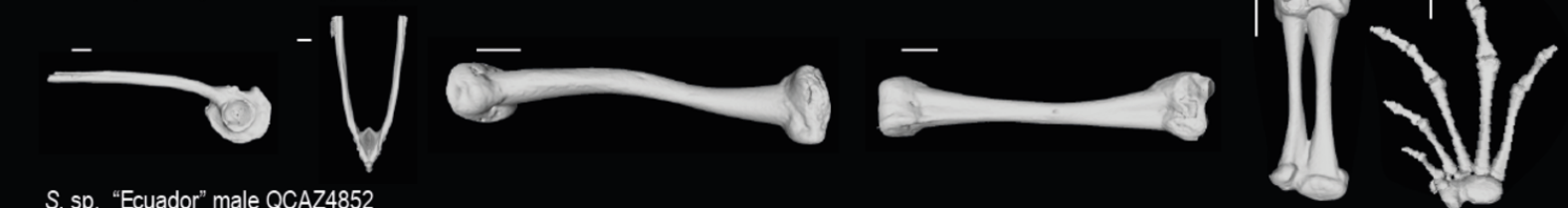
S. salseri male Paratype AMNHN89813

S. zombie sp. nov. male Paratype MNHN-RA-2020.0089

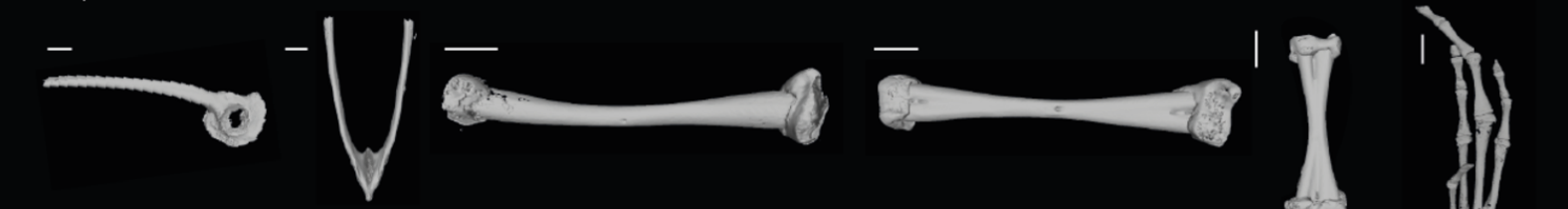*S. ajuricaba* sp. nov. female Paratype INPA-H35751

S. mesomorphus sp. nov. male paratype SMNS12077

S. sp. "Ecuador" male QCAZ4852

femur
tibio-fibula

S. sp. "Juami" male MCP13775